Masters Theses

Student Theses and Dissertations

Fall 2011

Visual inspection and ground penetrating radar investigation of the historical Pulaski County Poor Farm Cemetery

Ibrahim E. Ahmed

Follow this and additional works at: https://scholarsmine.mst.edu/masters_theses

Part of the Geological Engineering Commons

Department:

Recommended Citation

Ahmed, Ibrahim E., "Visual inspection and ground penetrating radar investigation of the historical Pulaski County Poor Farm Cemetery" (2011). *Masters Theses*. 5024.
https://scholarsmine.mst.edu/masters_theses/5024

VISUAL INSPECTION AND GROUND PENETRATING RADAR INVESTIGATION

OF THE HISTORICAL PULASKI COUNTY POOR FARM CEMETERY

by

IBRAHIM ELSHIEKH AHMED

A THESIS

Presented to the Faculty of the Graduate School of the

MISSOURI UNIVERSITY OF SCIENCE AND TECHNOLOGY

In Partial Fulfillment of the Requirements for the Degree

MASTER OF SCIENCE

in

GEOLOGICAL ENGINEERING

2011

Approved by
Neil L. Anderson, Advisor
Stephen Gao
Leslie Gertsch

ABSTRACT

This thesis is a comprehensive summary of the geotechnical investigation of the Historical Pulaski County Poor Farm Cemetery, southeast Waynesville, Missouri. This research demonstrates that unmarked graves in an abandoned historical cemetery can be located using visual site inspection and ground penetrating radar techniques.

During the course of these investigations, multiple visual site inspections of Pulaski County Poor Farm Cemetery were conducted and ground penetrating radar data were acquired. Based on the visual site inspections and the interpretation of ground penetrating radar data, a total of one-hundred and fifty-one (151) graves were identified; eighty-seven (87) of the graves were mapped using visual site inspection techniques; sixty-four fifty (64) were identified based on the analysis of the ground penetrating radar data. A report was submitted to the Pulaski County Historical Society, recommending that markers (wooden crosses) be placed on each identified grave.

The visual site inspections and ground penetrating radar investigation were successful and proved to be useful methods for detecting abandoned graves.

ACKNOWLEDGMENTS

A special thank you goes to my advisor, Professor Neil Anderson, who supported me throughout this research. Neil has not only been a great source of academic help, but also a very great friend and mentor. I also thank my committee members, Drs. Stephen Gao and Leslie Gertsch for their valuable suggestions.

I thank the S&T Department Chair, Dr. Ralph Flori, and the Head of the Geological Engineering Program Dr. Norbert Maerz, for their support. I also appreciate the faculty and staff of the Department of Geological Sciences and Engineering who made my stay at the university fruitful and enjoyable. In particular, I thank former S&T graduate student, Dr. Oleg Kovin, for collaborating in solving many scientific problems and creating a warm atmosphere in the office. A special note of appreciation is extended to S&T graduate student Mr. Evgeniy Torgashov who provided valuable insight into the ground penetrating radar (GPR) technique. I am also very thankful for the assistance and direction I received from Ms. Paula Cochran.

I am very exceedingly grateful to my wife Dalya and my daughters Roba and Reyna and my son Mohamed, for their support and incredible patience.

I thank the Missouri University of Science and Technology for awarding me a Chancellor's Fellowship so that I might pursue my PhD degree in geological engineering.

Finally, I thank my God for giving me the patience and ability to complete this thesis. Without him, I would not be where I am today.

TABLE OF CONTENTS

LIST OF ILLUSTRATIONS

LIST OF TABLES

1. INTRODUCTION

1.1. SUMMARY OF THESIS ORGANIZATION

This thesis is divided into eight chapters. Chapter one is the introduction. Chapter two is focused on the visual site inspection of Pulaski County Poor Farm Cemetery, southeast Waynesville, Missouri. Chapter three is an overview the ground penetrating radar (GPR) technique, including discussions of the dielectric permittivity (constant), diffraction, resolution, and energy loss or attenuation. GPR data acquisition, including the antenna selection, setup parameters, and the transfer the GPR data to a PC, is covered in chapter four. In chapter five, GPR data processing is discussed, complete with references to the Radan software used to process the GPR data. Chapter six is focused on the electrical resistivity tomography investigation (ERT). Chapter seven focuses on the interpretation of the GPR and ERT data acquired at the Pulaski County Poor Farm Cemetery. Conclusions and recommendations are presented in chapter eight.

1.2. OVERVIEW OF CHAPTER ONE

This chapter is divided into seven subsections. Subsection 1 is a summary of the thesis organization. In subsection 2, overview of chapter one is presented. Subsection 3 is focused on the statement of problem. In subsection 4, graves and coffins are covered. Subsection 5 is focused on the Pulaski County Poor Farm Cemetery restoration project. In subsection 6, Missouri S&T's involvement in the restoration project is discussed. Subsection 7 covers the objectives of the Missouri S&T investigative team.

1.3. STATEMENT OF PROBLEM

In June 2010, the Pulaski County Historical Society asked Dr Anderson if his graduate students willing to help restore the Pulaski County Poor Farm Cemetery. At that

time Dr Anderson asked for a brief description of the site. The Pulaski County Historical Society said the site was approximately 200ft x 200ft, covered by a lot of vegetation and surrounded by a wire fence. The Society was in the process of removing most of the vegetation and wanted to know the exact locations of the graves so that markers could be erected on each grave site. Dr Anderson asked the author to be in charge of the investigation of the Pulaski County Poor Farm Cemetery as part of the author's MS research. Dr Anderson asked the author to conduct a visual site inspection, a ground penetrating radar investigation, and an electrical resistivity tomography investigation, in order to locate and map unmarked graves.

This is not a simple process. The work plan consisted of the following:

Step 1. Collect as much background information about the Pulaski County Poor Farm Cemetery as possible.

Step 2. Get much information as possible about this particular cemetery's burial practices (types of coffins, coffin sizes, depth of the coffin, and spacing between the coffins).

Step 3. Look at other similar case studies, if other people investigated other cemeteries in Missouri, so the author can really understood the problems.

Step 4. Conduct a visual site inspection.

Step 5. Acquire ground penetrating radar (GPR).

Step 4. Acquire electrical resistivity tomography (ERT) data.

Step 6. Interpret the entirety of the data set and map locations of all unmarked graves.

1.4. PULASKI COUNTY POOR FARM

The study site, the Pulaski County Poor Farm Cemetery, is located on the Pulaski County Poor Farm (Figure 1.1). The "Pulaski County Poor Farm" was originally owned by Pulaski County; the property is now privately owned. The Pulaski County Poor Farm

was established in 1874, and used for the care of those in the County who were not mentally, physically, or financially able to care for themselves. Some were old and weak and senile. Some were crippled physically and other were blind (Pulaski County Historical Society, 1987). A few children were taken from their parents and placed there because of neglect. Many poor Pulaski County residents were buried in the Pulaski County Poor Farm Cemetery.

1.5. THE PULASKI COUNTY POOR FARM CEMETERY

According to an article in the Waynesville Daily Guide posted on August 17, 2010, the Pulaski County Poor Farm Cemetery was established around 1874 and closed in 1957. The Pulaski County Poor Farm Cemetery is located in southeast Waynesville Missouri beside the Spring/Superior road about 22 miles west of Rolla, Missouri (Figure 1.1). More than one hundred people are reported to have been buried in the Pulaski County Poor Farm Cemetery.

There are few headstones (only one still stands) on the Pulaski County Poor Farm Cemetery site, probably because it was too expensive to place stone markers on the graves. As a consequence, no one knows either the exact number of graves or the locations of the graves. The cemetery is now being maintained by Pulaski County Historical Society. The Pulaski County Historical Society asked Missouri S&T to help locate graves on the site so that markers could be placed at appropriate locations.

1.6. GRAVE SITES AND COFFINS

There is not much information about coffins used by the persons who ran the Pulaski County Poor Farm Cemetery. However, the Pulaski County Historical Society told the author the dead were almost certainly buried in inexpensive wooden coffins. During the site inspections, the author determined that the graves in the Pulaski County Poor Farm Cemetery are oriented almost east-west, with the head facing to the east to

greet the rising sun on Judgment Day. The depths to the top of the coffins probably vary, but are thought to be typically about 2ft (based on analyses of the acquired GPR data). The length of atypical coffins appears to be about 6ft; the width appears to be about 2ft. The space between adjacent graves is typically 5ft.   In places, the soil overlying the graves is sunken (by up to 1 ft), probably as a result of decay and collapse of the wooden coffins. Visually identifiable sunken grave sites account almost 60% (87 of 151) of the unmarked graves identified by the author.
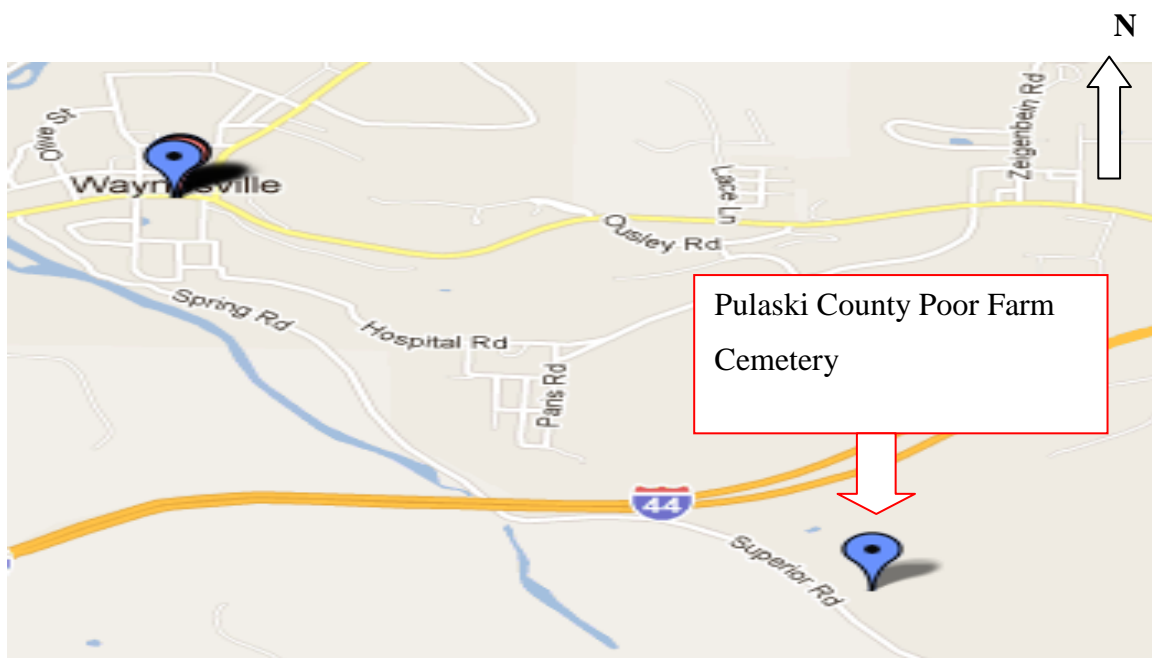
Figure 1.1. Map Showing the Location of Pulaski County Poor Farm Cemetery

1.7. THE PULASKI COUNTY POOR FARM CEMETERY RESTORATION PROJECT

The Pulaski County Poor Farm Cemetery restoration project is headed by the Pulaski County Historical Society. The main goal of Pulaski County Historical Society is to clean up, preserve and restore the Pulaski County Poor Farm Cemetery, to honor those buried there and allow a place for family members to gather and pay respects, and to

provide a place for the community to have a visible reminder of an overlooked part of Pulaski County history.

The Pulaski County Poor Farm Cemetery has been neglected and ignored for decades since being abandoned in 1957. On August 14, 2010 the US Navy Seabee's detachment at Fort Leonard Wood volunteered for a massive cleanup at the Pulaski County Poor Farm Cemetery. Their hard work and effort have put the Pulaski County Historical Society a lot closer to their vision on the finalized product of this restoration project.

1.8. MISSOURI S&T INVOLVEMENT IN RESTORATION PROJECT

The Pulaski County Historical Society approached to Missouri S&T and asked if we could help identify unmarked graves at the Pulaski County Poor Farm Cemetery. We took charge of this project and we did our investigations using visual inspection and GPR and ERT techniques on the site.

1.9. OBJECTIVE OF MISSOURI S&T TEAM

The objective of the Missouri S&T team was to accurately identify as many unmarked graves as possible on Pulaski County Poor Farm Cemetery site in southeast Waynesville, Missouri, so that the Pulaski County Historical Society could place markers (crosses) on each grave.

2. VISUAL SITE INSPECTION

2.1. OVERVIEW OF CHAPTER TWO

Chapter two is divided into eight subsections. Subsection 1 is overview of chapter two. Subsection 2 is focused on the geographic location of the Pulaski County Poor Farm Cemetery study site. In subsection 3, a description of the study site before the initial clean up (clearing of vegetation) is presented. Subsection 4 is focused on the United States Navy Seabees clean-up day (brush cleaning). In subsection 5, description of the study area after clean-up is presented. Subsection 6 focuses on the visual inspection of the Pulaski County Poor Farm Cemetery site which include information about soil type, the peripheral fence, the locations of the traverses (laid out for visual site inspection and GPR acquisition purposes), and the significance and nature of the "sunken" ground. Subsection 7 focuses on the few remaining graves markers and the unmarked graves of the Pulaski County Poor Farm Cemetery. In subsection 8, information about the few remaining headstones is presented.

2.2. GEOGRAPHIC LOCATION OF THE PULASKI COUNTY POOR FARM CEMETERY STUDY SITE

The study site, the Pulaski County Poor Farm Cemetery, is located southeast Waynesville, Missouri beside the Spring/Superior road about 22 miles west of Rolla, Missouri as shown in Figures 1.1 and 2.1. The Pulaski County Poor Farm Cemetery site is located on the outermost edge of the Rubidoux River flood plain (Figure 2.1 and 2.2). The study site may be occasionally subjected to flood waters that would deposit layers of silt and/or sand throughout the area. The cemetery is located on private property and is unmarked except for few headstones and an old wire fence that is still standing in places. The Pulaski County Poor Farm Cemetery was farmland. The cemetery, as it stands, September 12th, 2010 is located on private properties and is completely unmarked. The

Pulaski County Poor Farm Cemetery site located about 800ft far from the Rubidoux River.
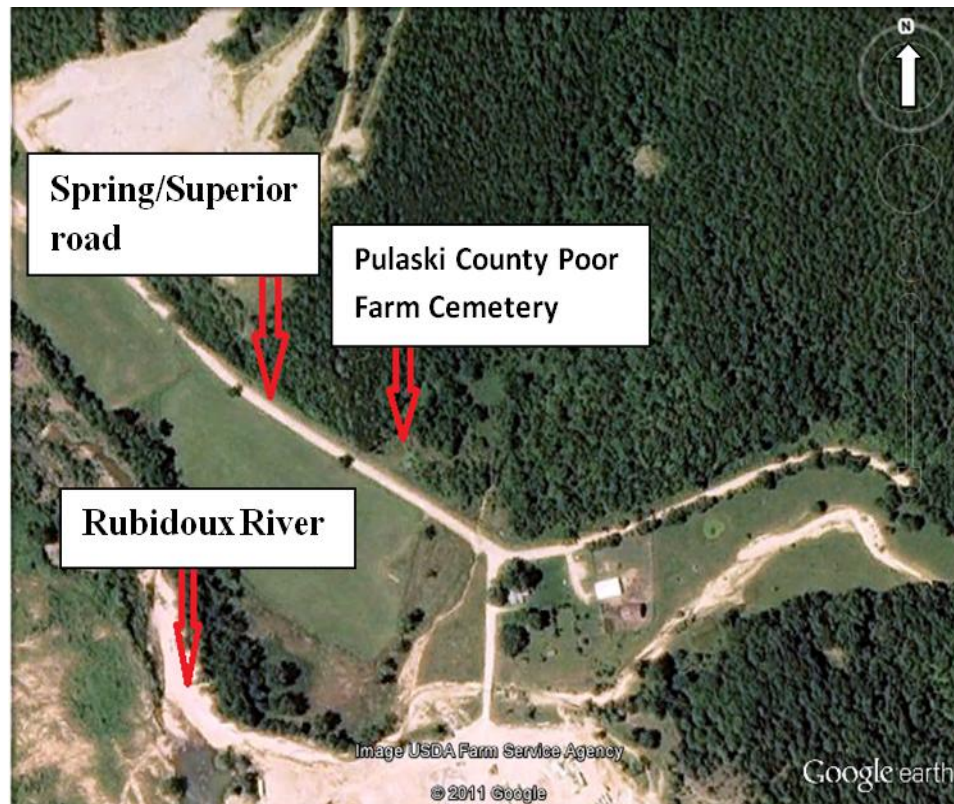
Figure 2.1. Google Earth Map of the Pulaski County Poor Farm Cemetery

2.3. DESCRIPTION OF THE STUDY SITE BEFORE THE INITIAL CLEAN-UP

Figures 2.2 and 2.3 show the Pulaski County Poor Farm Cemetery site before the initial clean up (brush cleaning; August 14th, 2010). The site was covered by trees, bushes, rocks and a few headstones. The Pulaski County Historical Society asked the United States Navy Seabees volunteers to clean up Pulaski County Poor Farm Cemetery site as part of their restoration effort.

Figure 2.2. Main Gate at Front of Cemetery

Figure 2.3. Old Fence Around Cemetery

2.4. THE UNITED STATES NAVY SEABEES CLEAN-UP DAY (BRUSH CLEARING)

On August 14, 2010, about one month prior the first Missouri S&T crew visit, a group of volunteers from United States Navy Seabees cleared vegetation from the Pulaski County Poor Farm Cemetery site in support of restoration efforts headed by the Pulaski County Historical Society.

Figures 2.4 and 2.5 are photographs of United States Navy Seabees clearing trees and vegetation from the cemetery site. After the Navy group completed their work, the site was suitable for visual site inspection and ground penetrating radar investigations with the objective of detecting and mapping old historical graves within the Pulaski County Poor Farm Cemetery site.

Figure 2.4. United States Navy Seabees Clearing the Site

Figure 2.5. United States Navy Seabees Removing a Large Tree

2.5. DESCRIPTION OF THE STUDY AREA AFTER CLEAN-UP

The photograph in Figure 2.6 illustrates conditions when the Missouri S&T crew first visited the site. The Pulaski County Poor Farm Cemetery had mostly been cleared of trees and brush prior to our arrival on the first day of the GPR survey (September 12, 2010), but many obstacles such as trees, shallow roots, rocks, and sunken ground remained, making it difficult to perform a proper GPR survey. As part of the initial visual site assessment, a base map was made of all the obstacles (trees, tree roots, sunken ground) that could adversely affect GPR data acquisition (Figure 2.12, 2.13 and 2.14).

2.6. VISUAL INSPECTION OF THE PULASKI COUNTY POOR FARM CEMETERY SITE

Since September, 12, 2010 the author has visited the Pulaski County Poor Farm Cemetery site five times in an effort to fully inspect the site. During the first visit, three important things came to the author's attention: soil type, the fence and the significance and nature of the "sunken" ground (subsidence above graves).

2.6.1. Soil Type. The soil on the Pulaski County Poor Farm Cemetery site is a mixture of sand and silt. These soils presumably were deposited as the result of the flooding of Rubidoux River and movement of the river back and forth across the valley. The site located just immediately outer edge of the floodplain. Houses nearby are at the same elevation, suggesting that the river does not flood regularly, and the site about 800ft away from the river (Figure 2.1). The type of the soil is very important from the perspective of GPR surveying. More specifically, GPR does not work well in clayey soil, but usually does work well where the soils are sandy and/or silty.

2.6.2. A Fence. The Pulaski County Poor Farm Cemetery site is more-or-less surrounded by a rusted wire fence that has collapsed in places. Laura Huffman (Pulaski County Historical Society), who is in charge of the restoration project, said "The fence almost certainly represented the outer edge of the cemetery" (as all markers and sunken ground lie within the boundaries of the old fence). When the author and Laura walked around the outer side area of the fence, there was no evidence of occurrence of the graves like sunken ground (subsidence above graves) or headstone markers. This indicated that all the graves of the Pulaski County Poor Farm Cemetery are probably located within the fenced area.

2.6.3 Depressions or Sunken Ground. The most important features discovered on the Pulaski County Poor Farm Cemetery site were the many depressions (sunken ground) on the site. These depressions do vary slightly in terms of size, but are arranged in rows and are oriented parallel to one another. What make these depressions important in this research is that each of these depressions is almost certainly indicative of the presence of a grave.

2.6.4. GPR Traverses. The author used a measuring tape and laid out 48 traverses on the Pulaski County Poor Farm Cemetery site (Figure 2.7). Starting from southwest corner of the site to the northeast, the length of each traverse is about 100ft, depending on accessibility. The interval spacing between each adjacent traverse was 2ft apart. Figures 2.7 and 2.8 show the 48 GPR traverses which were laid out across the Pulaski County Poor Farm Cemetery site, these traverses run from Southwest to Northeast with 2ft intervals between adjacent traverses. Collectively these traverses cover

the entire Pulaski County Poor Farm Cemetery. Starting from station "0", the author walked along each traverse and mapped all indentations (depressions; sunken ground), trees, tree roots, headstones, etc.

Figure 2.6. Uneven Ground, Trees, Tree Roots and Branches

2.6.5. The Significance and Nature of the "Sunken" Ground (Subsidence Above Graves). The expression "sunken ground", as used herein, refers to the visible depressions that are observed at many locations within the confines of the cemetery. These depressions were almost certainly caused by the degradation of the wooden coffins and human remains, and the collapse of the overlying soil. On the Pulaski County Poor Farm Cemetery site the depression of the sunken ground varies typically between 0.5ft and 1ft in depth. The centers of many of the depressions are about five feet apart indicating most the graves were spaced at about five-foot intervals. In many of the sunken grave sites, small trees have taken root. Typically, the depressions are about 6ft in

length and 2ft in width (consistent with burial practices as described by the Pulaski County Historical Society). Figures 2.9, 2.10 and 2.11 show three examples of depressions (subsidence above graves) on the Pulaski County Poor Farm Cemetery site. Figure 2.9 shows that the length of depression is about 6ft, the width is about 2ft and depth is about 1ft. The volume of this depression is approximately 10ft3.

   2.6.6. The Base Map. After all the sunken ground, trees and tree roots on the Pulaski County Poor Farm Cemetery site were mapped, a final base map was created to show all these natural features on the site. The trees and tree roots were mapped, because the author did not want to misinterpret the GPR signatures of tree roots as graves. Figures 2.13, 2.14 and 2.15 show the base map of the Pulaski County Poor Farm Cemetery site. On the base map the location of the trees, tree roots and sunken ground is shown. The depressions (sunken ground) are oriented almost east to west.
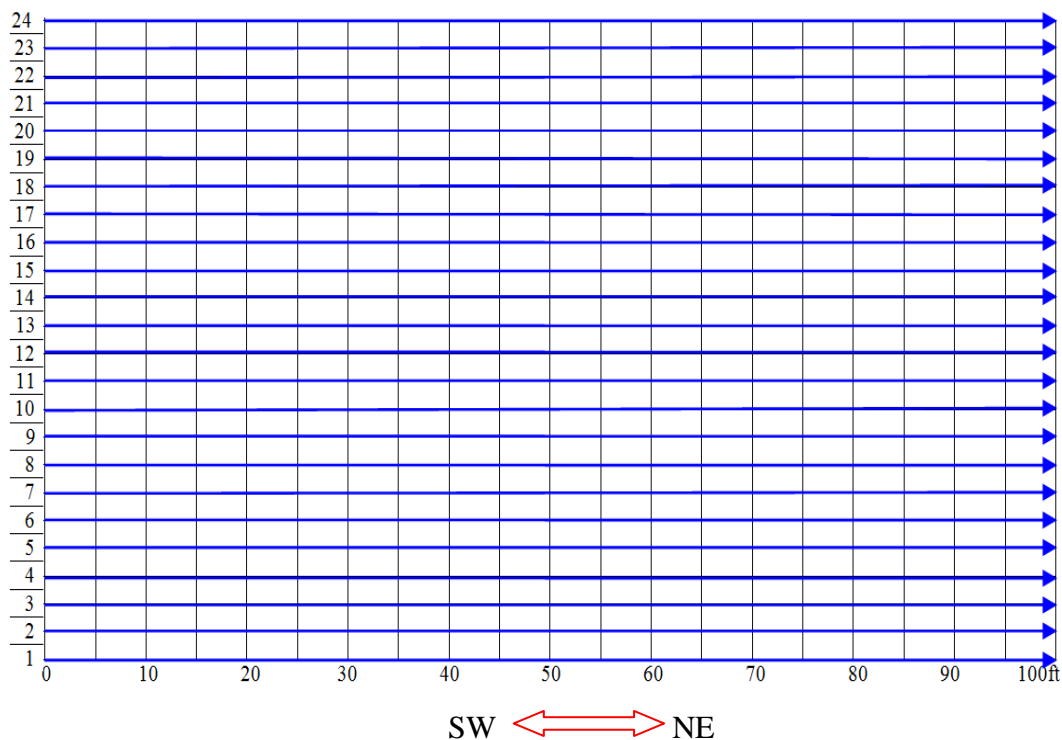
Figure 2.7. Map [1/2] of GPR Traverses (1-24)

Figure 2.10 shows the length of depression is 6.3ft, the width of the depression is 2.2ft and depth is 1.1ft. The volume of this depression is 6.3ft X 2.2ft X 1.1ft which equal to 12.25ft^3. This volume is approximately equal to the estimated volume of the original coffins.
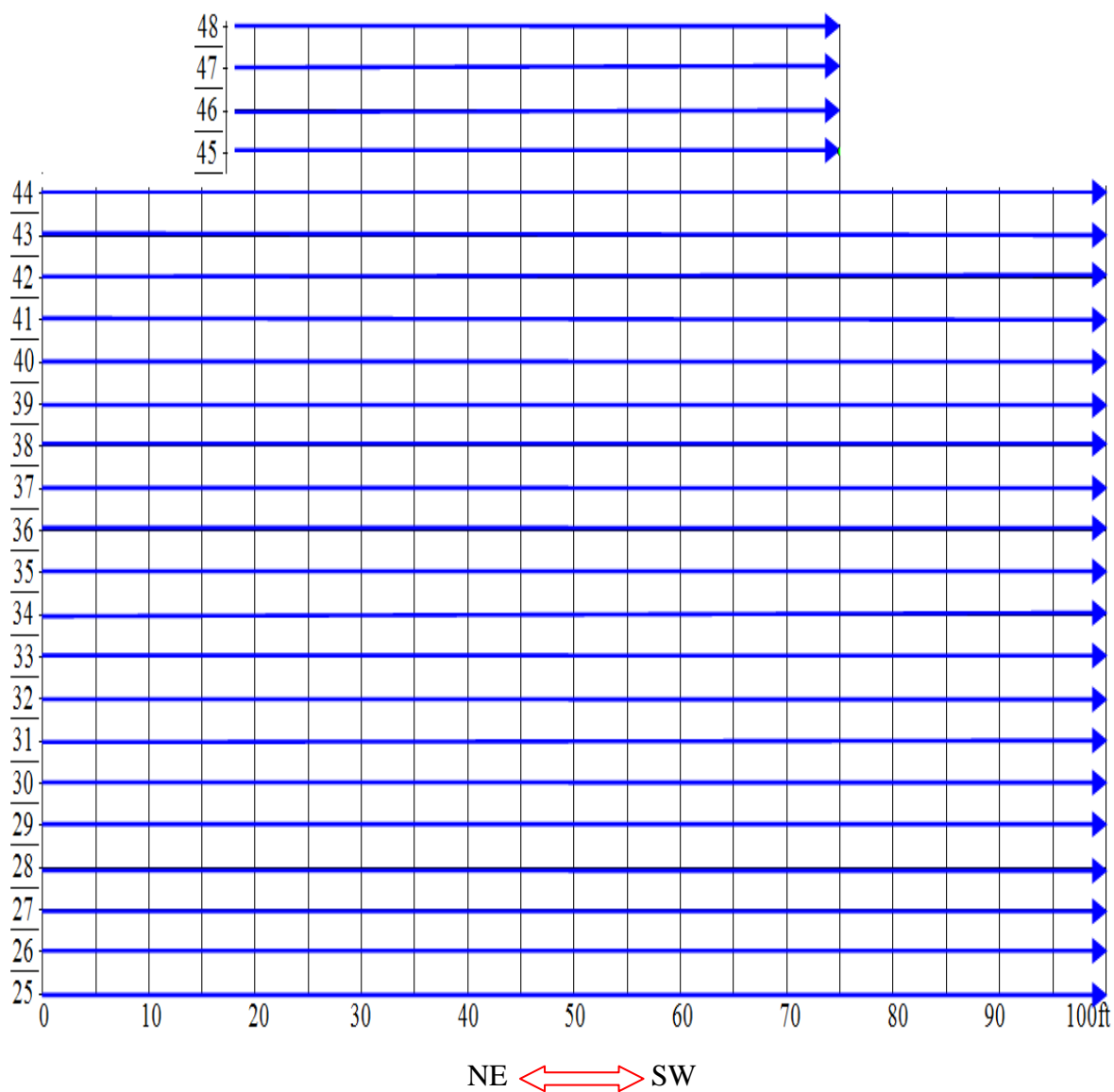
Figure 2.8. Map [2/2] of GPR Traverses (25-48)

All of the visually identifiable depressions (sunken ground) on the Pulaski County Poor Farm Cemetery site were mapped. Each indentation is presumed to correspond to a grave. The sunken ground is believed to be caused by the deterioration of the bodies and the coffins. The depressions are oriented almost east to west (Figures 2.13, 2.14 and 2.15).
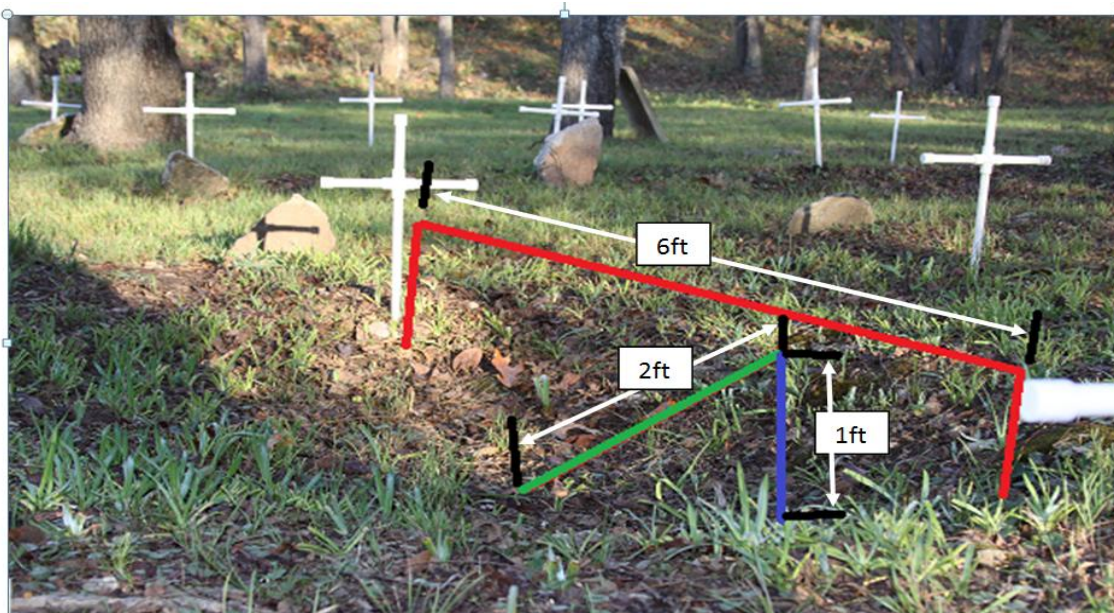
Figure 2.9. Typical Depression on the Site
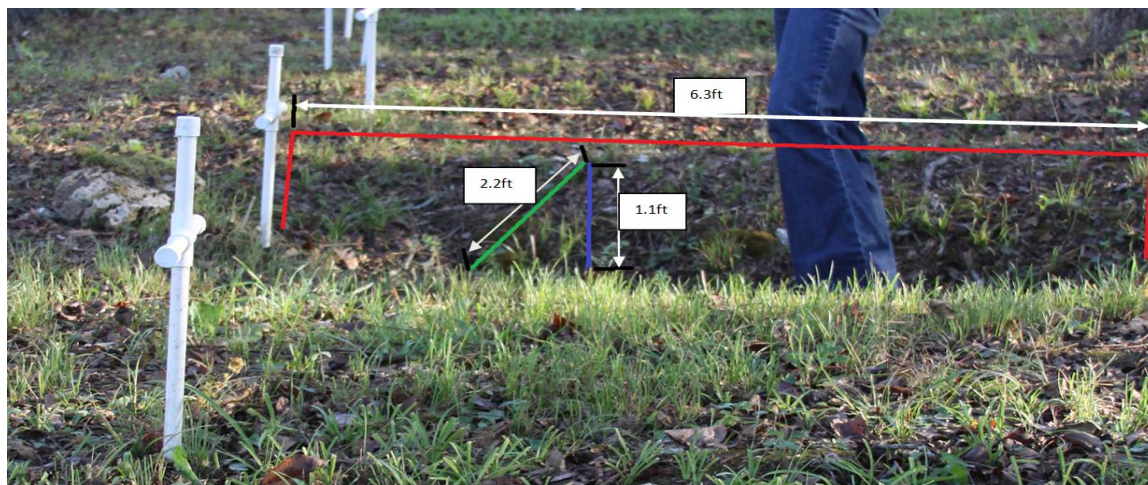
Figure 2.10. Typical Depression on the Site

Figure 2.11. Rocks and Sunken Ground

In this photo, a few rocks can be seen. These may have been used as grave markers at one time. Also, sunken ground is imaged on the photograph.

2.7. THE FEW REMAINING GRAVE MARKERS AND UNMARKED GRAVES OF THE PULASKI COUNTY POOR FARM CEMETERY

On the Pulaski County Poor Farm Cemetery many of the graves are difficult to identify, either because they were never marked, or because the grave markers have decayed, been removed, or been destroyed. Some graves were definitely marked headstones, as a few were found randomly dispersed on the site. Figures 2.15 and 2.16 show the only still-stand headstone marker and a non-standing headstone marker, respectively.

2.8. HEADSTONES

When the S&T crew walked across the Pulaski County Poor Farm Cemetery site looking for clues about the locations of unmarked graves, it did find two old headstones. One

was dated 2/12/1905 (Figure 2.15); and other one was dated 6/17/1912 (Figure 2.16). This indicates that the Pulaski County Poor Farm Cemetery is at least 106 years old.
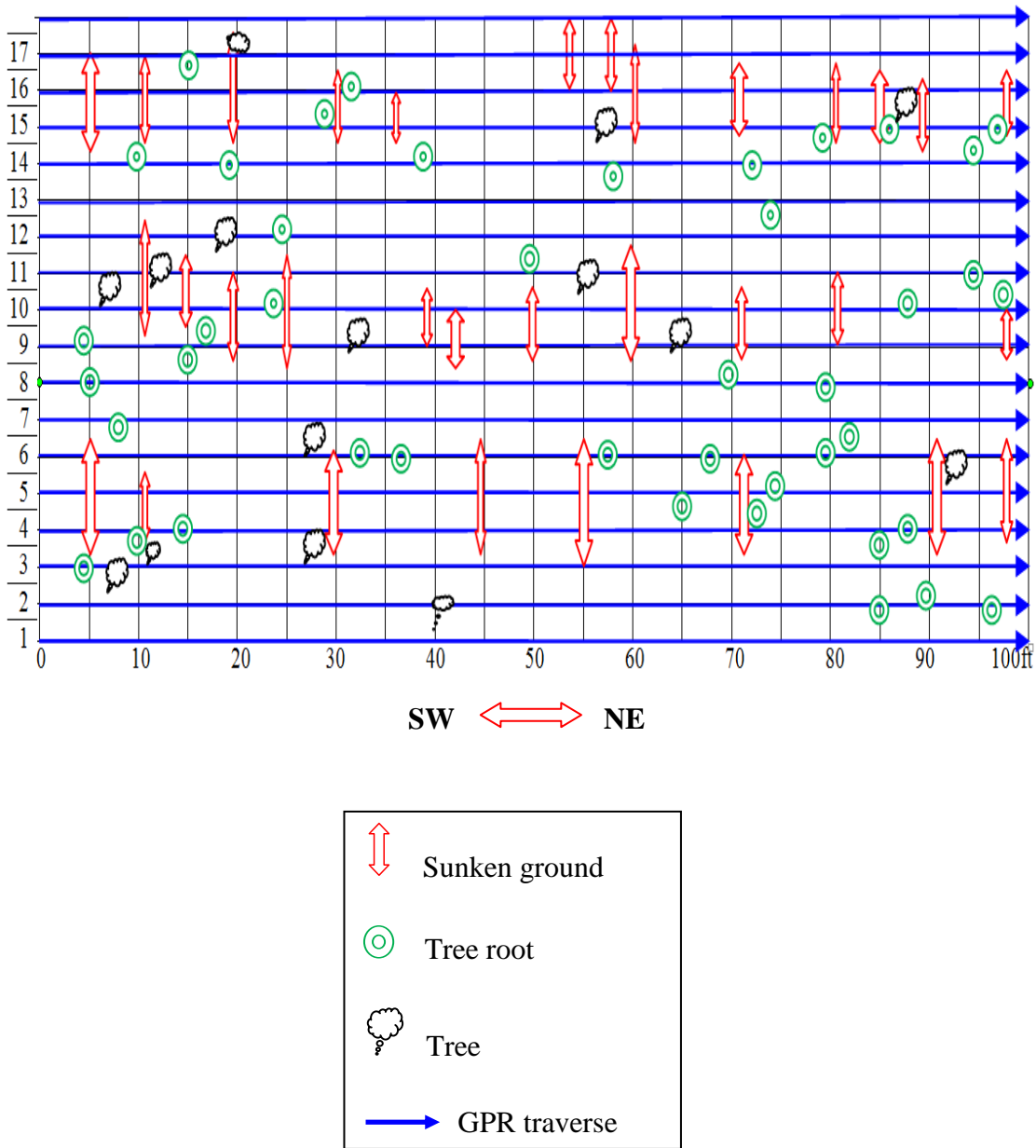
Figure 2.12. Base Maps [1/3] of Pulaski County Poor Farm Cemetery
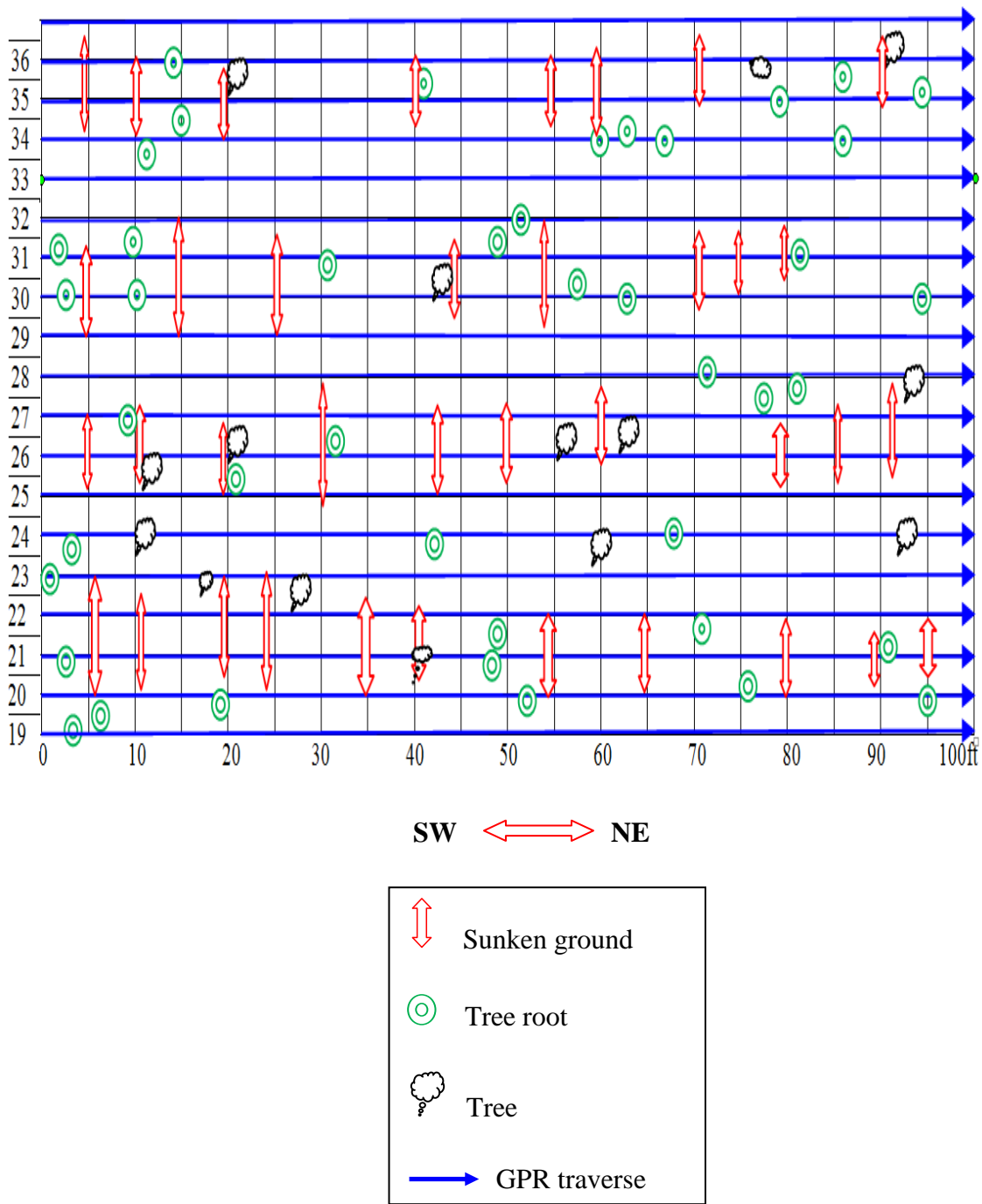
Figure 2.13. Base Maps [2/3] of Pulaski County Poor Farm Cemetery
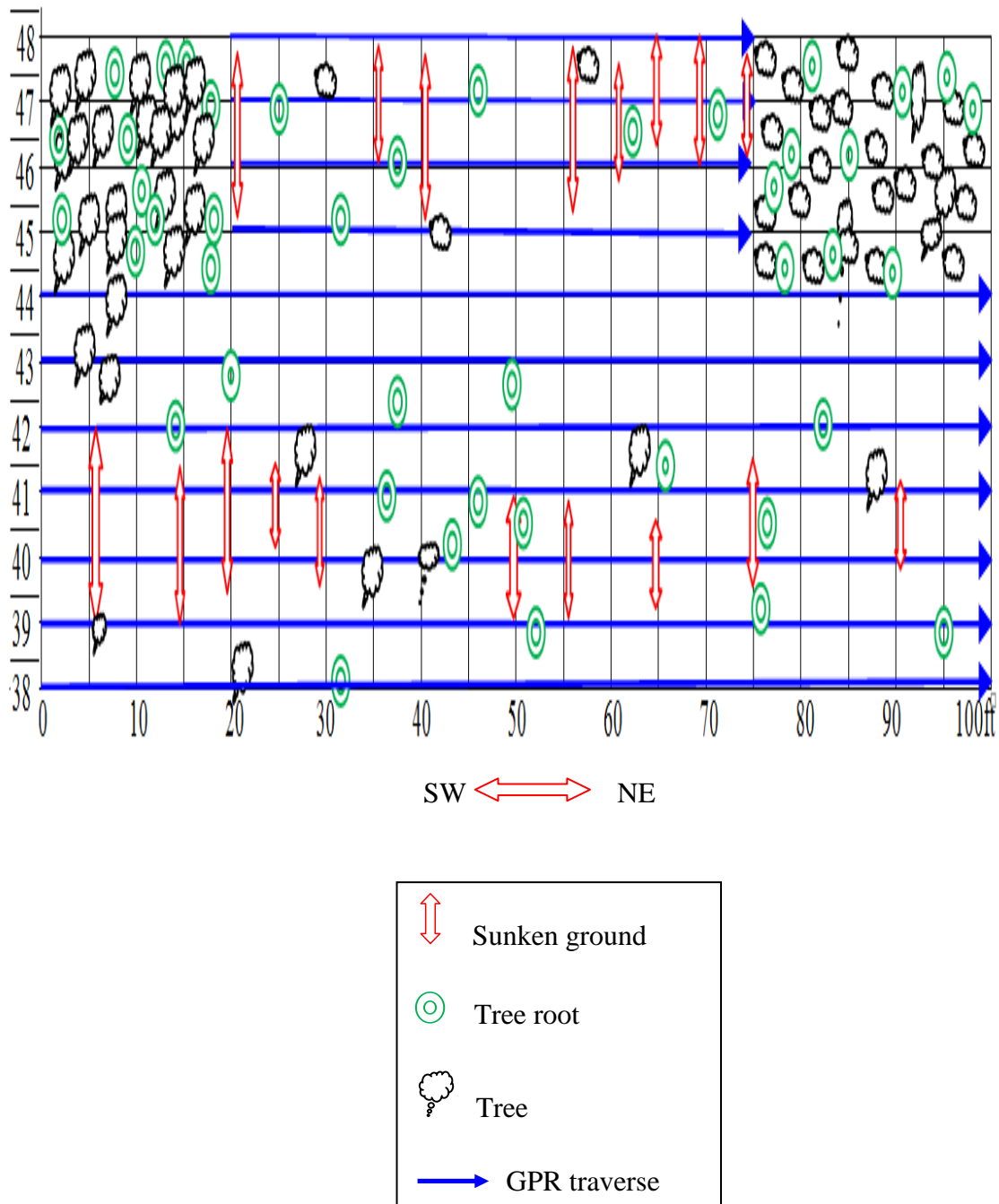
Figure 2.14. Base Maps [3/3] of Pulaski County Poor Farm Cemetery

Figure 2.15. Still-Standing Headstone Dated 2/12/1905

Figure 2.16. Non-Standing Headstone Dated 6/17/1912

3. GROUND PENETRATING RADAR (GPR)

3.1. OVERVIEW OF CHAPTER THREE

This chapter is divided into eight subsections. Subsection 1 is overview of chapter three. In subsection 2, a brief overview of the ground penetrating radar (GPR) method is presented. In subsection 3, the terms "trace length", "velocity of propagation" and "depth of investigation" are discussed. Subsection 4 is focused on the term "dielectric permittivity". In subsection 5, the concept of "diffractions" is presented. In subsection 6, "reflection and transmission coefficients" are covered. Subsection 7 is focused on the depth estimation and finally in subsection 8 "attenuation" or "energy loss" is discussed. As the monostatic GPR antenna is pulled, pushed or dragged across the surface of the feature that is being investigated, pulses of electromagnetic radiation (EM; radio wave frequencies) are emitted at predetermined distance intervals. This pulsed energy propagates into the subsurface with a velocity that is function of the dielectric permittivity of the material through which it is propagating. The reflected signals are recorded and stored digitally.

As shown in Figure 3.1, when down going pulse strikes an interface across which there is a change in dielectric permittivity, some of the energy is reflected back to the antenna where its arrival time and magnitude are recoded. Some of the energy is transmitted deeper into the subsurface as shown in Figure 3.1. The GPR system records the arrival time and magnitude of the reflected energy. If one knows the velocity with which this energy propagates, the depth to feature of interest can be calculated.

3.2. GROUND PENETRATING RADAR TECHNIQUE

A typical GPR system has three main components: a transmitter, a receiver and a control unit. Both transmitter and receiver serve as the GPR single antenna (monostatic)

of the GPR system (Figure 3.1). Conceptually the GPR tool is relatively simple, and very easy to work with.
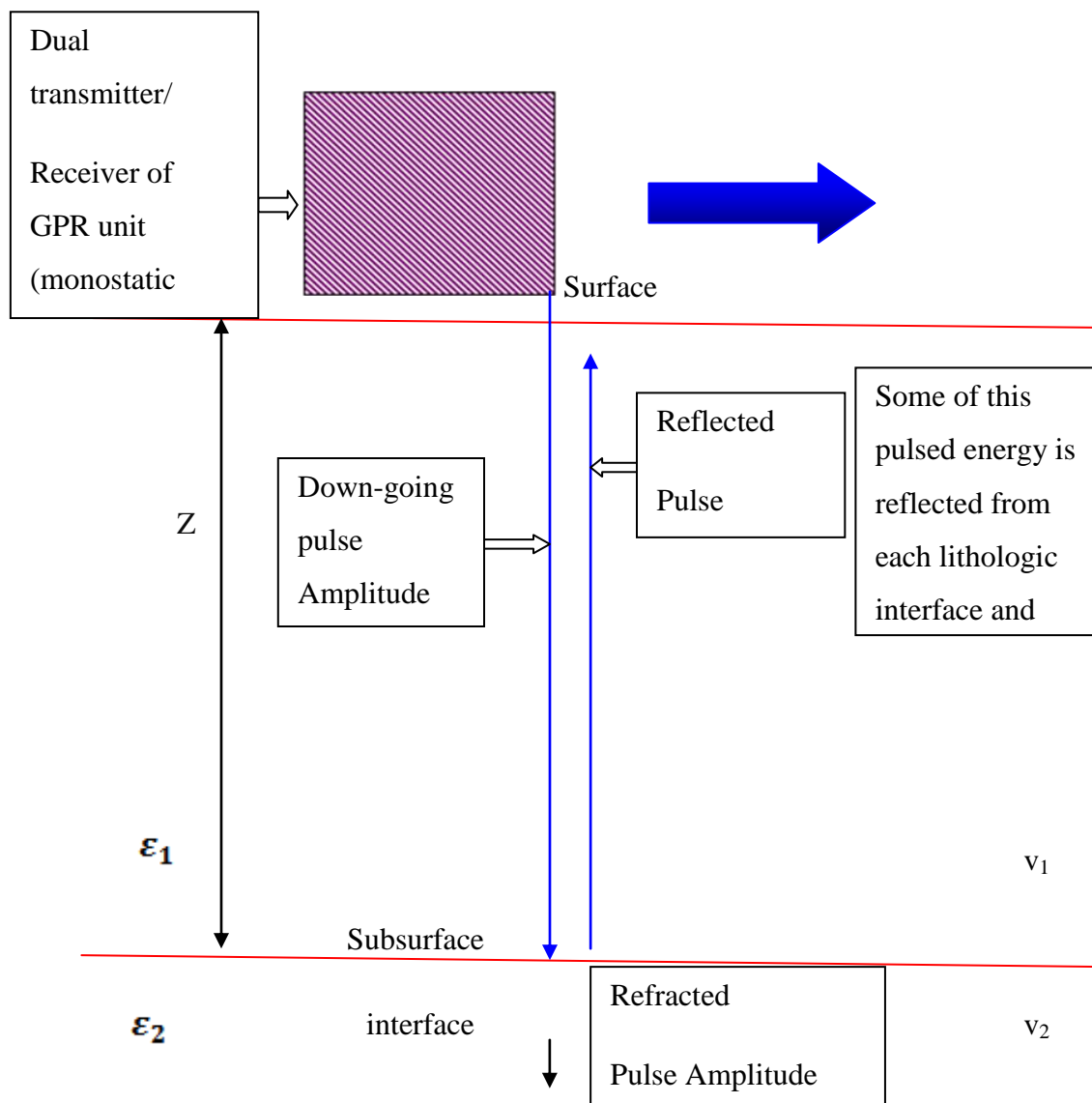
Figure 3.1. Down-Going Pulse, Refracted Pulse and Reflected Pulse

Where: ε_1 and ε_2 are dielectric permittivity of layer 1 and layer 2 respectively, v_1 and v_2 are the velocity of layer 1 and layer 2 respectively, v is the velocity of the with which this energy propagate into subsurface, C is speed of light in the vacuum, Z the depth to feature of investigation.

3.3. TRACE LENGTH, VELOCITY OF PROPAGATION AND DEPTH OF INVESTIGATION

The trace length is the length of the signal that is recorded after the pulse has been discharged. The propagation velocity of GPR pulse in the subsurface media is approximately C/ (ε_1)1/2, where C is the speed of light in vacuum ~ (0.3 m/ns) and ε_1 is the dielectric permittivity (constant). The dielectric permittivity of most dry and non-conducting rocks and soils vary between 5-15, and the propagation velocity in the ground is normally between about 0.077 m/ns and 0.134 m/ns (Basson 2000) (Table 3.1). The depth of investigation is function of the velocity propagation and the antenna used. However if the subsurface is highly conductive and if clay is present, the depth of investigation will be severely limited. GPR control unit can be used with different antenna utilizing different frequencies, normally varying between 10 and 2500 MHz. A lower frequency antenna provides for greater penetration depths but lower resolution. A higher frequency antenna provides for less depth of penetration but better resolution (Geophysical Survey System, Inc., 2006).

3.4. DIELECTRIC PERMITTIVITY (CONSTANT)

Dielectric permittivity is the capacity of a material to hold and pass an electromagnetic charge. It varies with a material's composition, moisture, physical properties, porosity, and temperature (Geophysical Survey System, Inc., 2006). For low radar frequencies (< 100MHz), the dielectric permittivity plays a dominant role in determining the velocity of a medium. For insulating materials such as dry rocks, dielectric permittivity alone determines the velocity of the EM wave. The effect of dielectric permittivity is seen in Figures 3.2 and 3.3. Figure 3.2 plots the velocity of an EM wave as a function of conductivity and frequency with a relative dielectric permittivity of 4. Figure 3.3 plots frequency vs. relative velocities with a constant resistivity of 50 Ω-m. It can be determined from Figure 3.3 for frequencies above 100

MHz, velocity is essentially independent of frequency and dependent only on the dielectric permittivity). Table 3.2 shows the list of relative dielectric constants and velocities for some earth materials (Annan and Cosway, 1992). Dielectric permittivity is primary factor influencing the speed of electromagnetic radiation in earth materials at ground penetrating radar frequencies.

Table 3.1. Electrical Properties of Some Geological Media (Davis et al., 1989)

Material	Dielectric Constant	Velocity (m/ns)	Attenuation (dB/m)
Air	1	0.3	0
Distilled Water	80	0.033	0.002
Fresh Water	80	0.033	0.1
Sea Water	80	0.01	1,000
Dray Sand	3-5	0.15	0.01
Saturated Sand	20-30	0.06	0.03-0.3
Limestone	4-8	0.12	0.4-1
Shale	5-15	0.09	1-100
Silt	5-30	0.07	1-100
Clay	4-40	0.06	1-300
Granite	4-6	0.13	0.01-1
Salt (dry)	5-6	0.13	0.01-1
Ice	3-4	0.16	0.01

Table 3.2. Relative Dielectric Constants and Velocities for Some Typical Earth
Materials (adapted from Annan and Cosway, 1992)

Material	Dielectric Constant	Velocity (m/ns)
Air	1	0.03
Sea Water	80	0.01
Dry Sand	3-5	0.15
Saturated Sand	20-30	0.06
Limestone	4-8	0.12
Silts	5-30	0.07
Granite	4-6	0.13
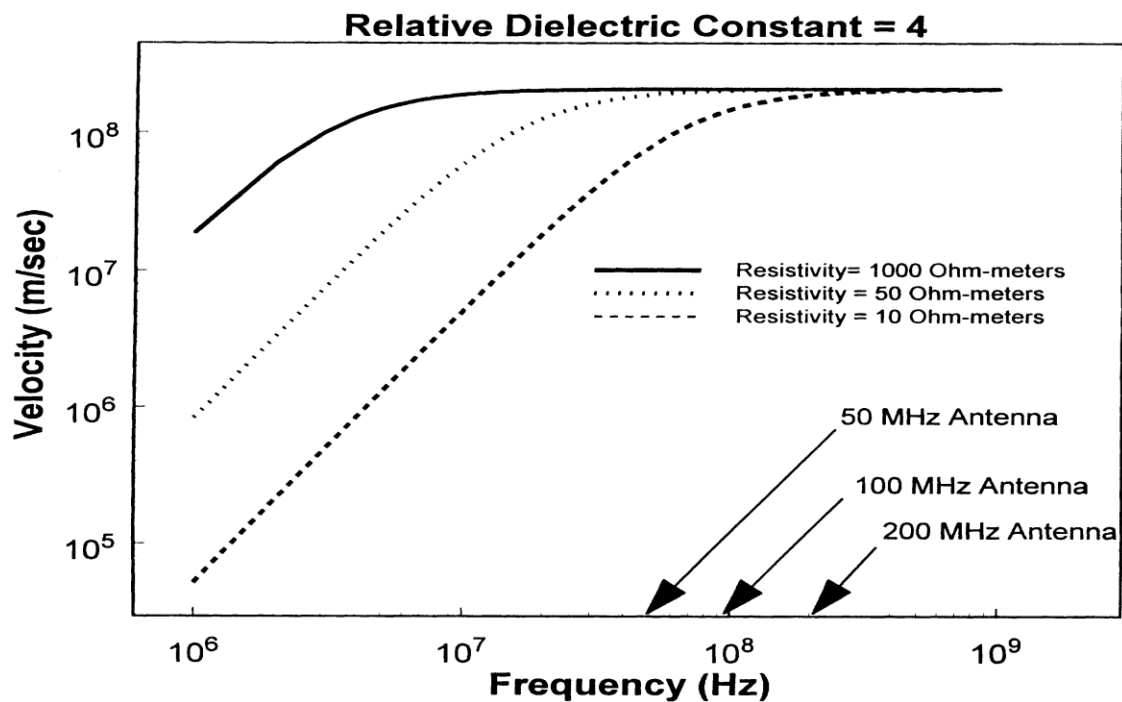
Figure 3.2. EM Wave Velocity Plotted as a Function of Soil Resistivity with a Relative
Dielectric Permittivity (Constant) of 4

Resistivity = 50 Ohm-meters
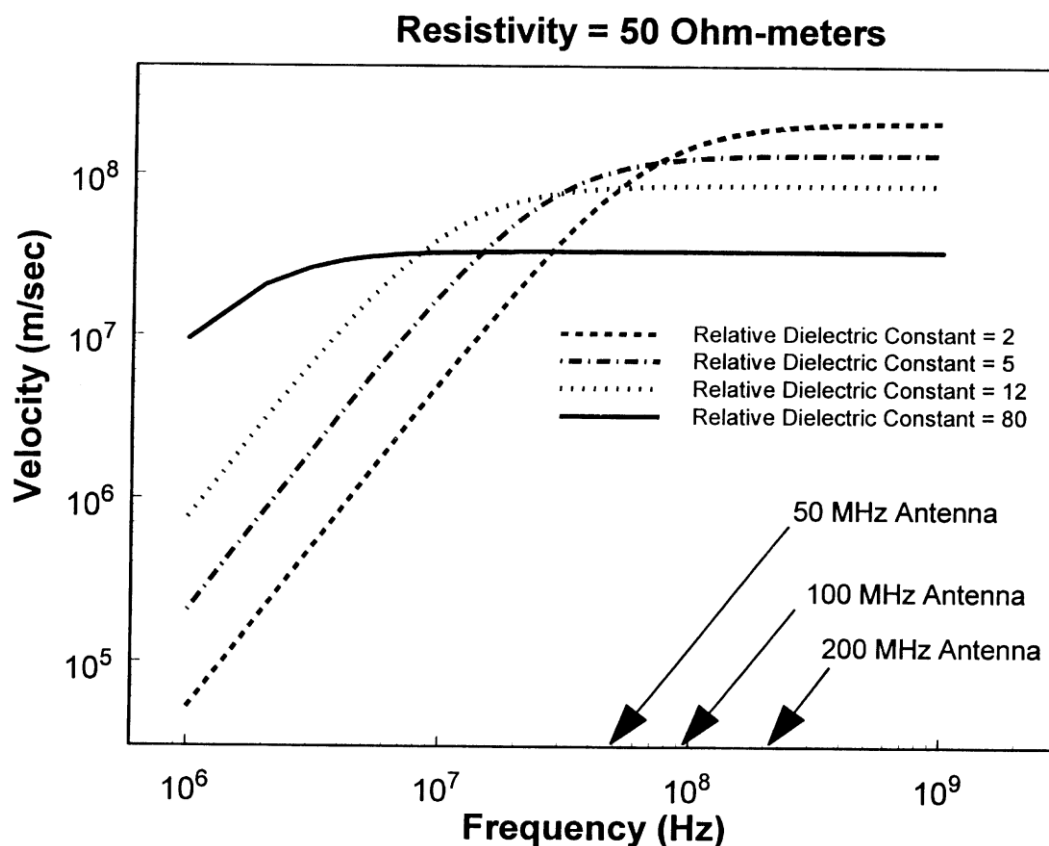
Figure 3.3. EM Wave Velocity Plotted as a Function of Relative Dielectric Permittivity for a Material with a Resistivity of 50 Ω m

3.5. DIFFRACTIONS

Diffractors are phenomena that cause electromagnetic waves in the beam of a directional antenna to spread out (the bending of wave energy around obstacles without obeying Snell's Law; an event that occurs at the termination of curved topped or steeply dipping reflectors that is characterized by a distinctive curved alignment) (GSSI SIR-3000 User's Manual., 2006). If a downward propagating GPR pulse encounters a curved surface, it octs as a point source and scatters energy back to the antenna, as shown on Figure 3.4.
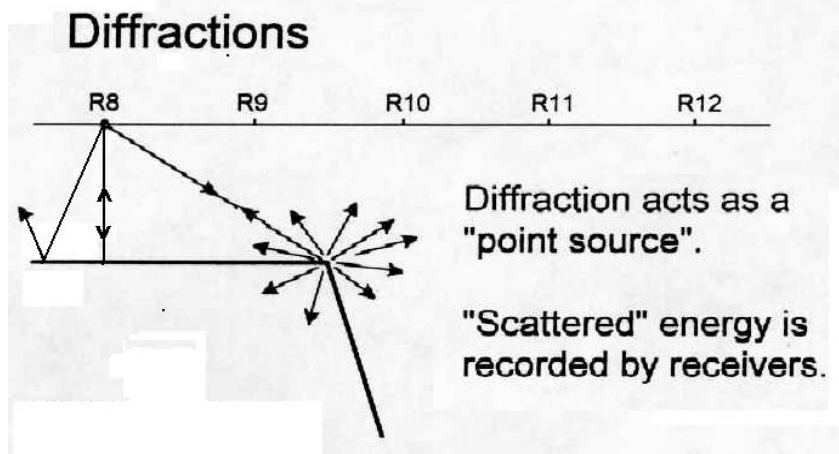
Figure 3.4. Diffractor Acting As a "Point Source" (GSSI SIR-3000 User's Manual, 2006)

On GPR data, the image of a coffin can look like the image of a large buried utility because both are characterized by prominent diffractions.(Diffractions are important when imaging buried utilities, because the small features we seek are often characterized on GPR data by prominent diffractions). These prominent diffractions can be removed via migration but usually we do not do so, because the diffractions highlight the features of interest. Prominent diffractions can be seen on Figure 3.5. The tops of the coffins in Figure 3.6 appear to be at depths of about 1ft, separately by 5ft intervals. This is similar to the situation expected at the study site.

3.6. REFLECTION COEFFICIENT

Dielectric permittivity differences between two adjacent layers cause the reflection or diffraction of the some EM energy while the remainder is transmitted into the underlying layer. Table 3.3 shows that the magnitude of a reflection is proportional to the different dielectric permittivity (constant) between two materials. This table further indicates that the greater the contrast between adjacent media, the stronger the reflection.
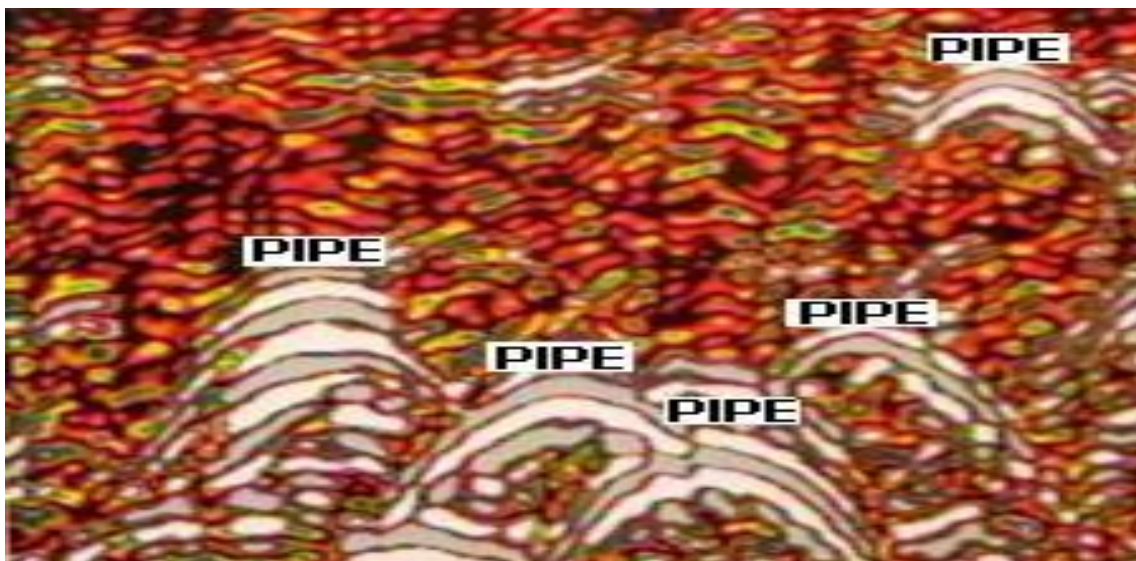
Figure 3.5. Prominent Diffractions Generated by Buried Utilities
(Federal Highway Administration (FHWA), 2007)
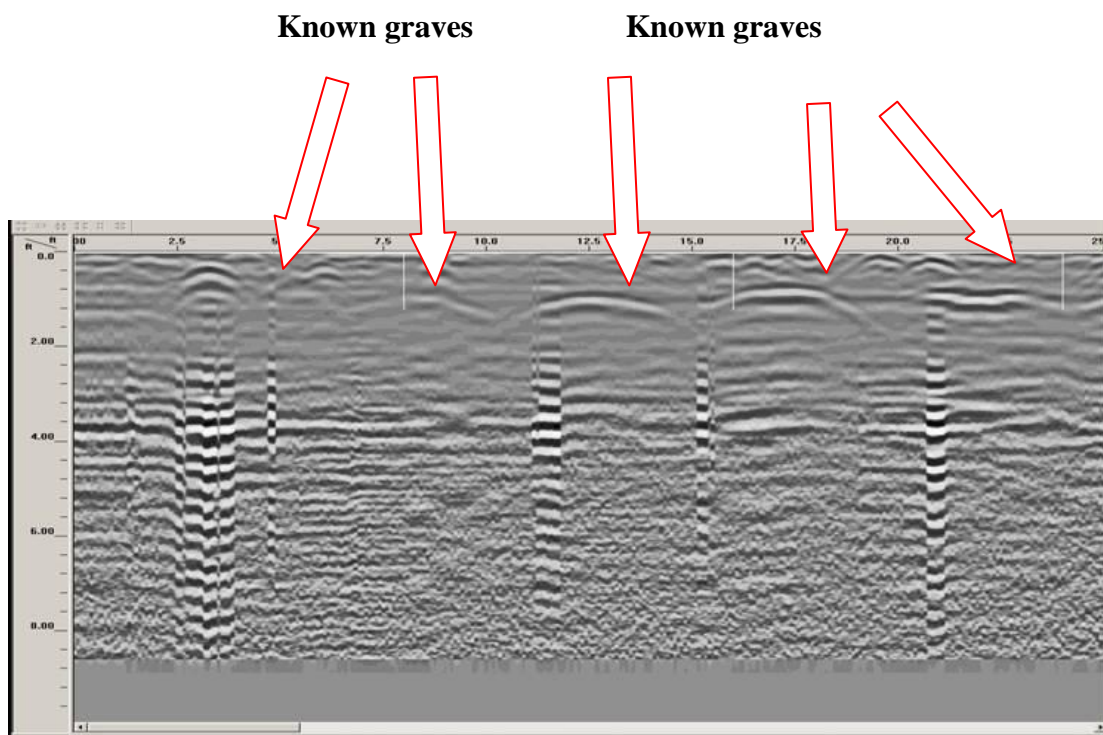
Figure 3.6. Ground-Penetrating Radar 2D Data Acquired Across Veterans Cemetery in
St. James

Table 3.3. Dielectric Permittivity (Constant) Contrasts Between Different Media and Resulting Reflection Strength (GSSI MN72-367 Rev. D, 2005)

Boundary	Dielectric Contrast	Reflection Strength
Asphalt-Concrete	Medium	Medium
Concrete-Sand	Low	Weak
Concrete deck-Concrete beam	None	No reflection
Concrete-Metal	High	Strong
Concrete-Water	High	Weak

Calculation of the reflection coefficient is simple when the dielectric permittivity (constant) increases or decreases across the interfaces (i.e., less than one-quarter of the wave length) (Baker et al., 2007). The velocity is inversely proportional to dielectric permittivity of the medium; therefore reflection coefficient (R) can also be calculated by using the dielectric permittivity, Equation (1).

$$R = (\sqrt{\varepsilon_1} - \sqrt{\varepsilon_2})/(\sqrt{\varepsilon_1} + \sqrt{\varepsilon_2}) \qquad (1)$$

Where ε_1 and ε_2 are dielectric permittivity of layer 1 and layer 2, respectively (Reynolds, 1997).

3.7. DEPTH CALCULATION

High frequency antennas are employed where resolution is of great importance; however, this is a trade off with depth of penetrating and vice versa. GPR penetration depth is a function of moisture content, salt content, number of reflection and scattering

centers, and the frequency of the EM wave (Maierhofer, 2003). Assuming a perfect dielectric medium, the arrival time can be converted into depth or thickness using Equation (2).

$$d = vt/2 \qquad\qquad (2)$$

Where, d = depth to the target (m).

   v = velocity of EM wave in a media (m/ns), and

   t = two-way travel time (ns).

3.8. ATTENUATION OR ENERGY LOSS

The magnitude of GPR energy diminishes as the function of distance travel due to several factors including geometric spreading, partial reflection and absorption. Attenuation is the loss or dissipation of energy as radio waves travel from the source through the subsurface. This is analogous to the loss of cell phone signal when driving a tunnel and it is dependent on the nature and thickness of the overburden on the tunnel. The signal detected by the receiver undergoes numerous losses during its transmission (Geophysical Survey Systems, Inc, 2006), as seen in Tables 3.4 and 3.5.

3.8.1. Ground Coupling Effect. This is the energy loss that occurs when there is an air interface between the transmitter/receiver antenna and the surface. The amplitude of the signal changes as it travels through the air media (transmission-coupling loss). This air interface also affects the signal on its return journey to the receiver (retransmission-coupling loss).

3.8.2. Geometric Spreading. As the sound moves away from the source, the area that the sound energy covers becomes larger and thus sound intensity decreases. This is referred to as geometric spreading, which is independent of frequency and plays a major role in sound propagation. Geometric spreading occurs as the EM energy propagates

away from the transmitter, resulting in the weakening of the radar signal. Although the radius increases further from the source the energy output does not increase; therefore, the energy per unit area reduced with time. Naturally occurring clays are as significant attenuators, and it is mostly concluded that GPR is not applicable in this environment. It should be noted that non clay but clay sized materials (i.e., fresh glacial rock flour) do not attenuate signal to the degree observed in naturally occurring clays; thus, it is not true to say that clay sized materials strongly attenuate GPR signal (it is the fraction of naturally occurring clay that is important) (Baker et al., 2007). Table 3.5 presents material loss for selected media.

Table 3.4. Attenuation and Electrical Properties of Various Materials
Measured at 100MHz Frequency   (Daniels, 2004)

Material	Attenuation (dB/m)	Dialectic Permittivity
Air	0	1
Asphalt: dry	2-15	2-4
Asphalt: wet	2-20	6-12
Clay: dry	10-100	2-6
Clay: saturated	10-100	15-40
Concrete: dry	2-12	4-10
Concrete: wet	10-25	10-20
Granite: dry	0.5-10	5
Granite: wet	2-5	7
Limestone: dry	0.5-10	7
Limestone: wet	10-25	8
Sand: dry	0.01-1	4-6
Sand: wet	10-100	10-30

Table 3.5. Typical Range of Loss for Various Materials at 100 MHz and 1 GHz
(Daniels, 1996)

Material	Loss at 100 MHz	Loss at 1 GHz
Clay (moist)	5-300 dB/m	50-3000 dB/m
Loamy soil (moist)	1-60 dB/m	10-600 dB/m
Sand (dry)	0.01-2 dB/m	0.1-20 dB/m
Ice	0.01-5 dB/m	1-50 dB/m
Fresh Water	0.1 dB/m	1 dB/m
Sea Water	1000 dB/m	1000 dB/m
Concrete (dry)	0.5-2.5 dB/m	5-25 dB/m
Brick	0.3-2.0 dB/m	3-20 dB/m

4. GPR DATA ACQUISITION

4.1. OVERVIEW OF CHAPTER FOUR

This chapter is divided into ten subsections. Subsection 1 is overview of chapter four. Subsection 2 is focused on the ground penetrating radar tool. In subsection 3, the GPR main control unit is discussed. Subsection 4 is focused on the survey wheel. In subsection 5, information about the 400 MHz antenna is presented. Subsection 6 is focused on booting-up and the display screen. In subsection 7, setup parameters of ground penetrating radar (GPR) are covered. Subsection 8 is focused on collecting data. In subsection 9, the transfer data to PC is presented, and finally in subsection 10 example of GPR data from the Pulaski County Poor Farm Cemetery site are shown.

4.2. GROUND PENETRATING RADAR

Ground penetrating radar (GPR) data were acquired on the Pulaski County Poor Farm Cemetery using a 400 MHz antenna. The locations of the traverses along which ground penetrating radar data were acquired are shown as Figures 4.1 and 4.2. The ground penetrating radar profiles were collected along traverses spaced at 2ft intervals beginning in the southwest corner of the study area running to the northeast corner of the Pulaski County Poor Farm Cemetery site. The ground penetrating radar data were collected in the parallel or unidirectional mode with the operator returning to the same zero (0) ft mark to start the next traverse profile. The ground penetrating radar data were collected from Southwest to Northeast. A total of 48 ground penetrating radar profiles were collected across the Pulaski County Poor Farm cemetery. Measuring tape was used to measure all 48 ground penetrating radar traverses. The tape was stretched from zero (0) ft mark to 100 ft.

In the following subsections, the author discuss sequentially: 1) the ground penetrating radar main control unit, 2) the survey wheel; 3) the antenna was selected, 4)

boot-up and the display screen and 5) data collection parameters. Ground penetrating radar data were acquired along a total of 48 traverses.

4.3. GPR MAIN CONTROL UNIT

The main control unit (SIR-3000) of GPR system was used to acquire a GPR data. In Figure 4.3, the main control unit (SIR-3000) was put on the survey cart and connected to the antenna.

SW ⟺ NE
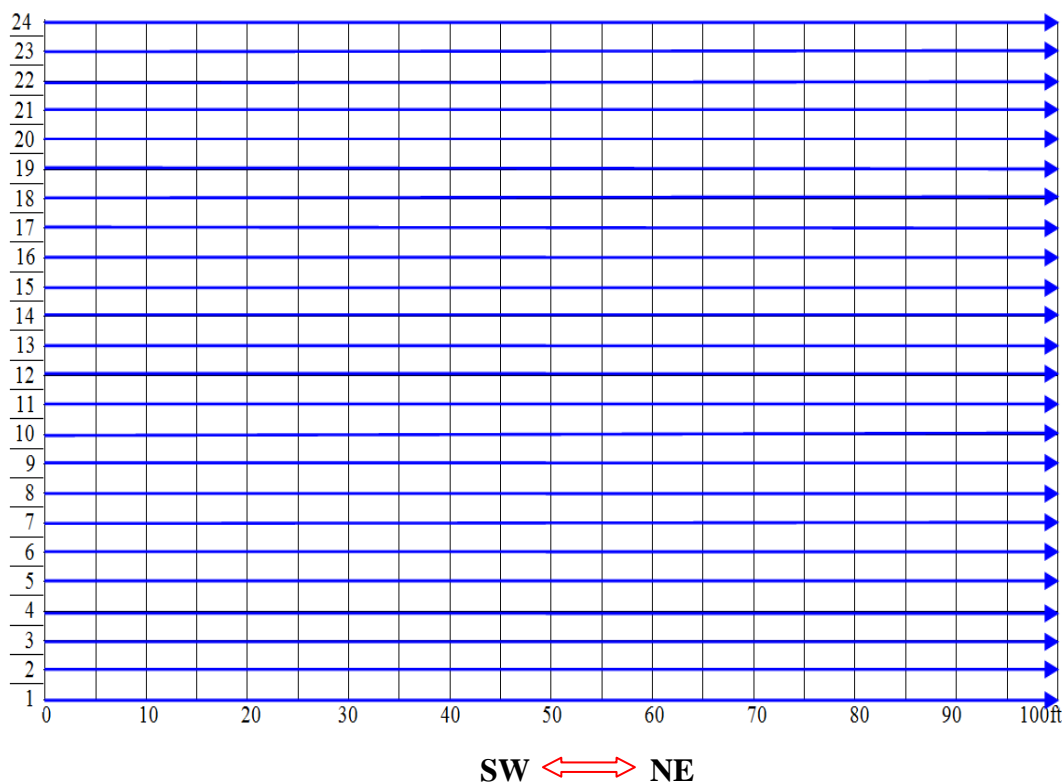
Figure 4.1. Map [1/2] of GPR Traverses (1-24)

The locations of GPR traverses 1–24 are shown in Figure 4.1. Each GPR profile started at the 0 ft mark, with the exceptions of traverses 45-48 which started near the 15 ft mark because dense brush was present near the 0 ft mark. Most of the traverses ended near the

100 ft mark. However, a few were terminated at shorter distances because heavy brush was encountered. The GPR traverses are 2 ft apart.
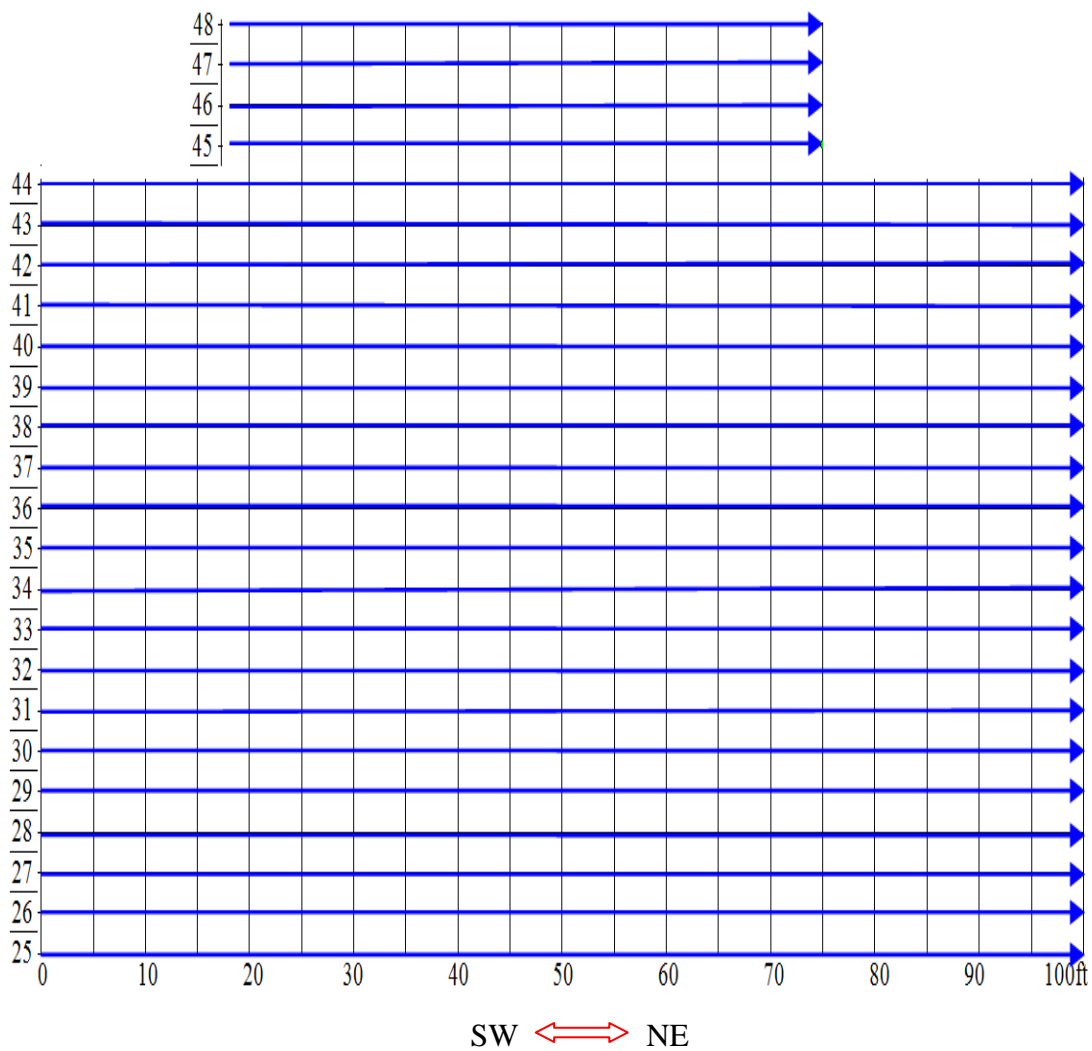
Figure 4.2. Map [2/2] of GPR Traverses (25-48)
(Ahmed and Anderson, 2010)

The locations of GPR traverses 25–48 are shown in Figure 4.2. Each GPR profile started at the 0 ft mark, with the exceptions of traverses 45-48 which started near the 15 ft mark

because dense brush was present near the 0 ft mark. Most of the traverses ended near the 100 ft mark. However, a few were terminated at shorter distances because heavy brush was encountered. The GPR traverses are 2 ft apart.

The main control unit of the GPR system (GSSI SIR-3000) is a lightweight, portable, single-channel ground penetrating radar system that is can be deployed for a wide variety of applications. The major external features of the control unit are the keypad, color SVGA video screen, connector panel, battery slot, and indicator lights. The video screen allows to view data in real time or in playback mode. It is readable in bright sunlight, although an optional sunshade for the unit is available. Figure 4.4 shows the front view of the control unit. The high-resolution screen allows a high-quality data display. The keypad on the front of the unit has fifteen (15) operation buttons and two indicator lights. Figure 4.5 shows rear connector panel offers variety hardware connectors to use the different types of antennas and copy data files to the external devices.
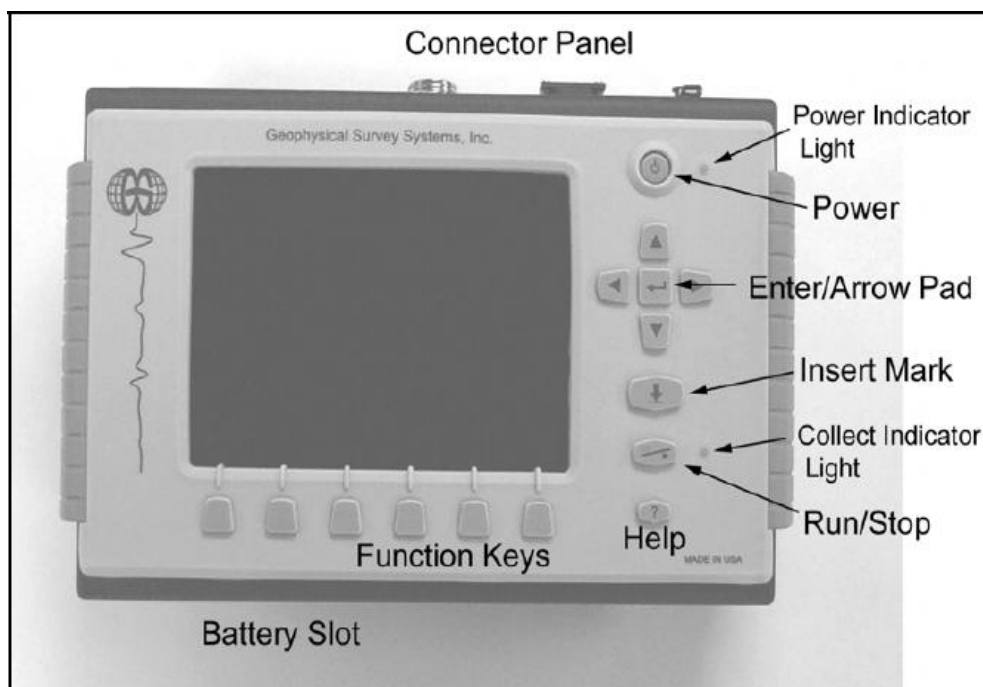
Figure 4.3. Front View of Control Unit
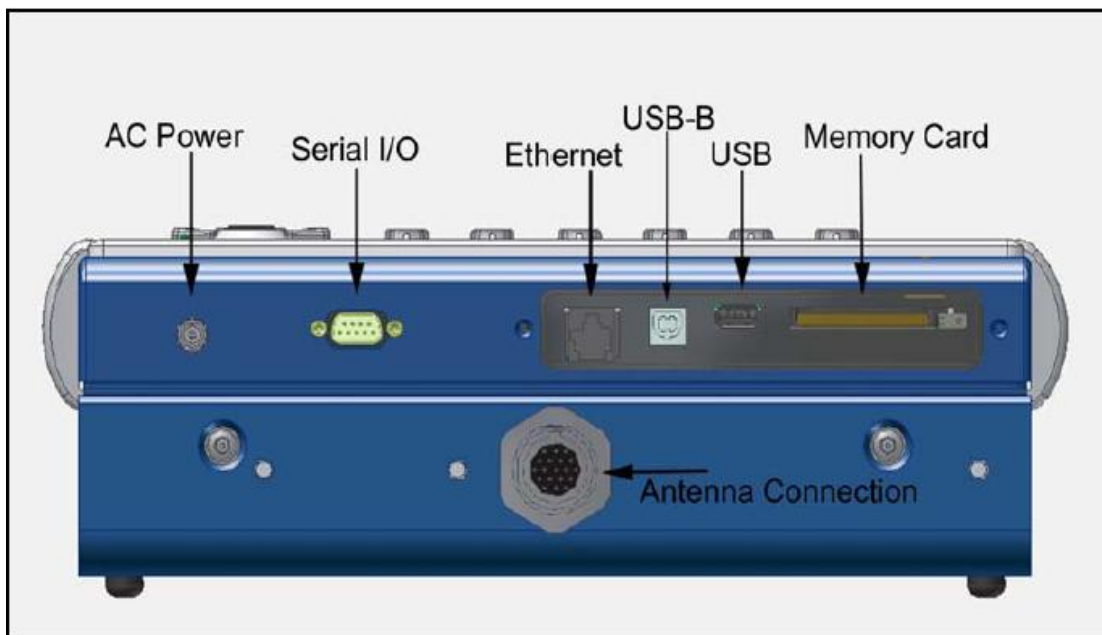
Figure 4.4. Rear Control Panel

4.4. SURVEY WHEEL

The GPR cart is coupled to a survey wheel. The survey wheel enabled the Missouri S&T crew to acquire GPR data at one inch intervals as the antenna was pushed along the traverses.. At the Pulaski County Poor Farm Cemetery site we acquired a GPR data along 48 traverses by using a survey cart. Figure 4.3 shows the survey cart.

4.5. ANTENNA 400 MHz

400 MHz antenna were employed. Using a 400 MHz antenna allowed us to image the subsurface to a depth of about 3m (10 ft) which was more than deep enough to image the casket targets. The GSSI, model 5103A has a center frequency of 400 MHz when measured in air. The 400 MHz is suited for archeology, engineering and environmental applications. According to GSSI this type of antenna has capability up

imaging the subsurface to 3 meters depth. The weight of the antenna is 5 kg (11 lbs) and the its dimensions are 12x12x6.5 in (30x30x17 cm)(Figure 4.6).

Figure 4.5. 400 MHz Antenna

4.6. BOOT-UP AND DISPLAY SCREEN

After the SIR-3000 boots up, the introductory screen with the words TerraSIRch, SIR-3000 Figure 4.7. There will be six icons positioned over the Function Keys. These six icons are TerraSIRch, Concrete Scan, Structure Scan, Utility Scan, Geology Scan and Quick 3D. During a GPR data acquisition we used the first mode (TerraSIRch). We used the TerraSIRch mode because it gives us complete control over all data collection parameters. Push the TerraSIRch button, after a moment, a screen divided into three windows and there will be a bar running across the bottom with commands above each of the 6 Function Keys.

Table 4.1. Various Antenna Frequency Applications
(GSSI SIR-3000 Users Manual, 2006)

Frequency	Sample Applications	Typical Max Depth Feet (meter)
1.6 GHz	Structural Concrete, Roadways, Bridge Decks	1.5 (0.5)
900 MHz	Concrete, Shallow Soils, Archaeology	3 (1)
400 MHz	Shallow Geology, Utility, Environmental, Archaeology	9 (3)
200 MHz	Geology, Environmental	25 (8)
100 MHz	Geology, Environmental	60 (20)

4.7. SET UP PARAMETERS

To acquire a GPR data there are many different parameters need to select. These parameters include dielectric permittivity; the value we selected is 8 because of dry soil. The depth of investigation we used 8ft which deep enough to image the casket should be shallower than 8ft depth. We select 400 MHz for radar choice. This GPR data was acquired in distance so we selected distance mode. Also samples 512 samples and 12 scans/ft.

4.8. COLLECTING DATA

GPR data were acquired along the traverses shown on Figures 4.8 and 4.9. In Figure 4.3 GPR data were acquired by bushing cart wheel attached to antenna and the

main control unit. Dr. Anderson is looking at GPR data has been acquired with attempt of visual inspecting the data quality and try to identify the anomalies.

Figure 4.6. Shows Introductory Screen with 6 Function Keys

4.9. TRANSFER DATA TO PC

The data collected from the Pulaski County Poor Farm Cemetery with easily be transferred to a PC for intensive processing in RADAN, by using a flash drive.

4.9.1. Plug in Memory Card. Remove the black plastic cover above the antenna connector and find the slot for the Compact Flash memory card. Insert the card into the slot and push gently until the square plastic button next to the slot pops up. There is only one right way for it to go in, so do not force it.

4.9.2. Turn on the SIR-3000. Connect a battery or AC power to automatically turn on the system. Select Utility Scan.

4.9.3. Open Transfer Submenu. In the output menu, highlight transfer and click "Right" bottom. Highlight flash and click Enter. "Select Files to Copy" (Figure 4.11).

4.9.4. Select Files and Transfer. Highlight each file to be transferred and press Enter to put a check in the box next to the file name. Press Right key option to transfer files. This moves each file from the internal memory to the flash drive. A USB memory "stick" Can also be used. These devices plug into the USB master port on the back of theSIR-3000 and can be used as a data taxi just like Flash cards. They are more durable than Flash cards, but one cannot collect data directly to them. First collect to the internal Flash card and then plug in one of those devices to transfer data to them. Then use the HD choice under the Transfer menu for these devices. The raw data folder containing the profile line data were transferred to the PC computer via the flash drive for further processing by using Radan 6.1 software.

Figure 4.7. Acquisition of GPR Data

Figure 4.8. Graduate Students Holding GPR Antenna for Data Acquisition

Figure 4.9. Quality Assurance and Identification of Anomalies
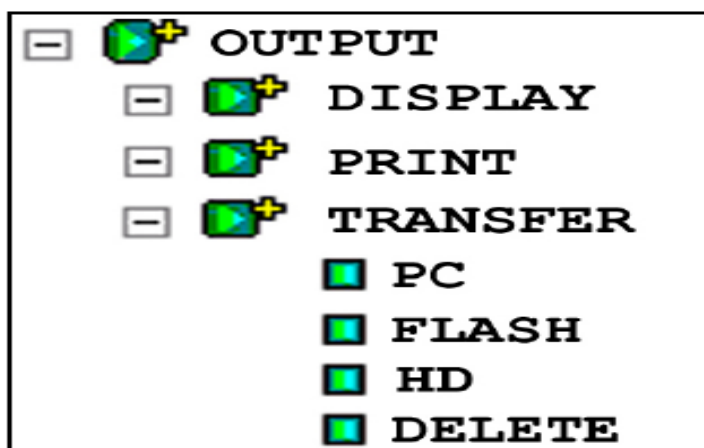
Figure 4.10. Transfer Data Menu
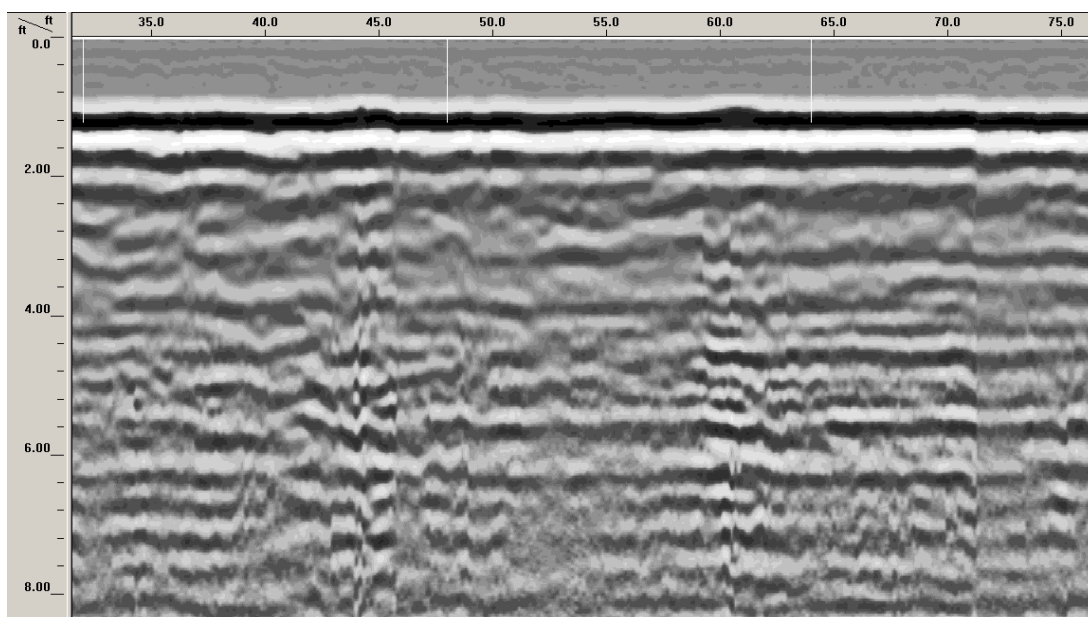
Figure 4.11. Ground-Penetrating Radar 2D Data Acquisition

5. GPR DATA PROCESSING

5.1. OVERVIEW OF CHAPTER FIVE

This chapter is divided into seven subsections. Subsection 1 is an overview of chapter five. Subsection 2 is focused on the overview of Radan software. In subsection 3, the main Radan module functions are described. Subsection 4 is focused on the rationale behind the processing GPR data. In subsection 5, the GPR data processing sequence used in this research is presented. In subsection 6 an example of poor farm cemetery GPR data processed is shown. In Subsection 7, GPR images acquired at the Veterans Cemetery in St. James Missouri is presented.

5.2. THE OVERVIEW OF RADAN SOFTWARE

According to the manufacturer of the Missouri S&T GPR system (GSSI), the Radan software was created to fill a GPR data processing need, and to provide both novice and experienced GPR users with processing capabilities using a windows XP Pro or Vista format, making the processing radar images easy. The Radan software package consists of a main module and add-on modules. The main Radan module (henceforth called Radan) provides all of the tools necessary to display, process, analyze, interpret and present ground penetrating radar data for most applications. (Geophysical Survey System, Incorporated, 1995, RADAN for Windows Manual).

5.3. RADAN MAIN MODULE FUNCTIONS

According to GSSI the main Radan module can perform the following functions:

1- Display multiple screens of radar data as linescan (color-amplitude plots), wiggle trace, or oscilloscope.

2- Manipulate color table and color transform parameters to enhance data display.

3- Edit file headers and distance markers.

4- Process individual files in Macro Programming Mode.

5- Process multiple files using Project Processing.

6- Modify or restore data gains.

7- Correct position (shift data scans along the time axis).

5.4. THE REASONS BEHIND PROCESSING GPR DATA

According to GSSI the GPR data processing should be done for the following reasons:

1- To remove unwanted signal (noise) from the data and thereby improve data interpretation.

2- To correct for geometric errors and provide more accurate spatial and depth interpretation.

3- To convert from time to depth and provide accurate information in depth sections.

4- To provide displays to you (and your clients) that is easier to understand than the raw data.

Data processing schemes should be designed to accomplish these overall objectives, and each processing step should be designed to fulfill a specific objective.

5.5. THE GPR DATA PROCESSING SEQUENCE

The following is sequence was used in this research to process the GPR data:

1- Open a GPR data file.

2- Horizontal scaling.

3- Display parameters setup

4- Surface position adjustment.

5- View and edit file header.

Before opening any data files, I selected the customize command in the view menu to set certain parameters essential for the processing, these include the source and output folders (directories) and the linear units (feet) for both horizontal and vertical scales.

5.5.1. Opening a GPR Data File. The Radan files were saved with the following format "*.dzt", this file can be easily opened after running Radan software by choosing file option "File > Open". The software defaults to the directory set as source. Either select the file you wish to input from the default source folder, or use the mouse to click onto the folder in which your file is stored. Click ok; file will open up on the screen. To review the data use the left or right scroll arrows. Then the file can be saved to storage media, such as the hard drive, CD or other media like flash drive after done of the processing.

5.5.2. Horizontal Scaling. Data may be modified by adjusting the Horizontal Scale using the Stacking, Skipping and Stretching functions. To do this, use the button or go to the Process menu and select Horizontal Scale (Figure 5.1).

Stretching: Select Stretching to expand the horizontal scale. The Stretching function will calculate the simple average of two adjacent scans (Figure 5.2).
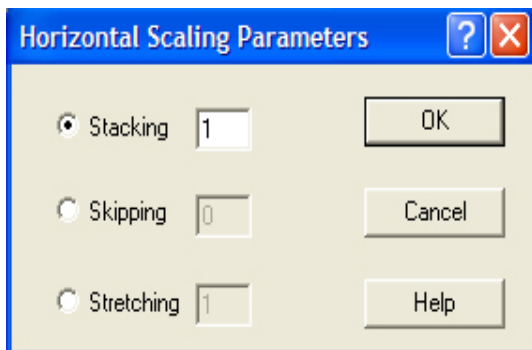

Figure 5.1. Shows Horizontal Scaling Parameters

5.5.3. Display Parameters Setup. The display options command under the view menu allows reviewing and modifying the display parameters for GPR data. There are four icons for different display formats: linescan, wiggle, o-scope, and 3-D as well as the print icon. Double-clicking on a display format icon will open the parameters dialog box for selected format as shown on Figure 5.3.

5.5.3.1. Linescan display parameters. Select the linescan icon to create a color-amplitude image of the data file as it loaded. The linescan parameters dialog box (Figure 5.2) can be opened by selecting the linescan icon in display parameters setup.

5.5.3.1.1. <u>Color table.</u> Color table is used to code the amplitude of each scan (i.e. the recorded radar signal) as shown in Figures 5.4 and 5.5. The user may choose one of the standard display color tables from a list of twenty-five. A color table represents the amplitude of the recorded radar signal mapped to different colors. The Pulaski County Cemetery GPR data were processed using table 17 as shown in Figure 5.5 which represent high-resolution (256 shades) gray scales.

5.5.4. Surface Position Adjustments. It is necessary to vertically adjust the position of the whole profile in the data window (adjust time-zero). The user may want the first positive peak of the direct wave from a ground coupled antenna to be centered at the top edge of the screen so that the ground surface will be at the top of the window (at Time Zero). This can be done using the correct position command in the process menu or by selecting the button. A corrected 0-position will give a more accurate depth calculation because it sets the top of the scan to a close approximation of the ground surface (Figure 5.6).

5.5.5. View and Edit the File Header. A header accompanies each data file and describes the setup of the radar system at the time of data collection. Some of this information can be edited to correspond to post-processing changes or for report generation. Also, the file header should include field information such as location, client, date, job number, surface material, or other information useful in characterizing a site. On the "File Header" menu all the parameters used during acquiring ground penetrating radar data can be well seen.
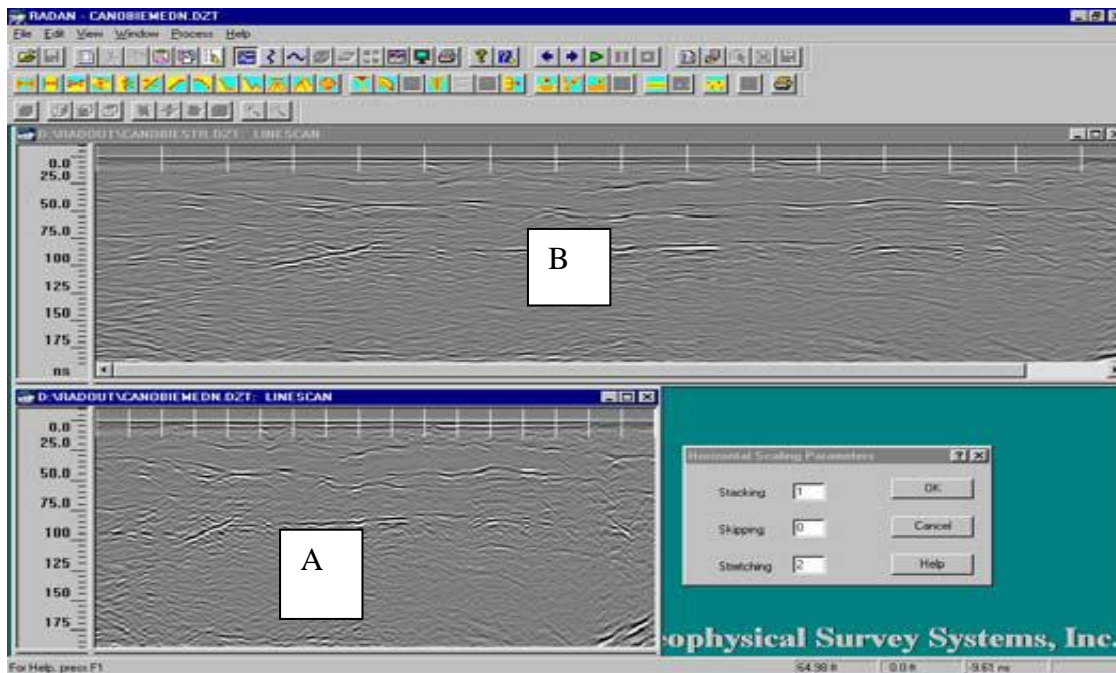
Figure 5.2. Display in Capture A Stretched by Factor 2 to Achieve Display in Capture B
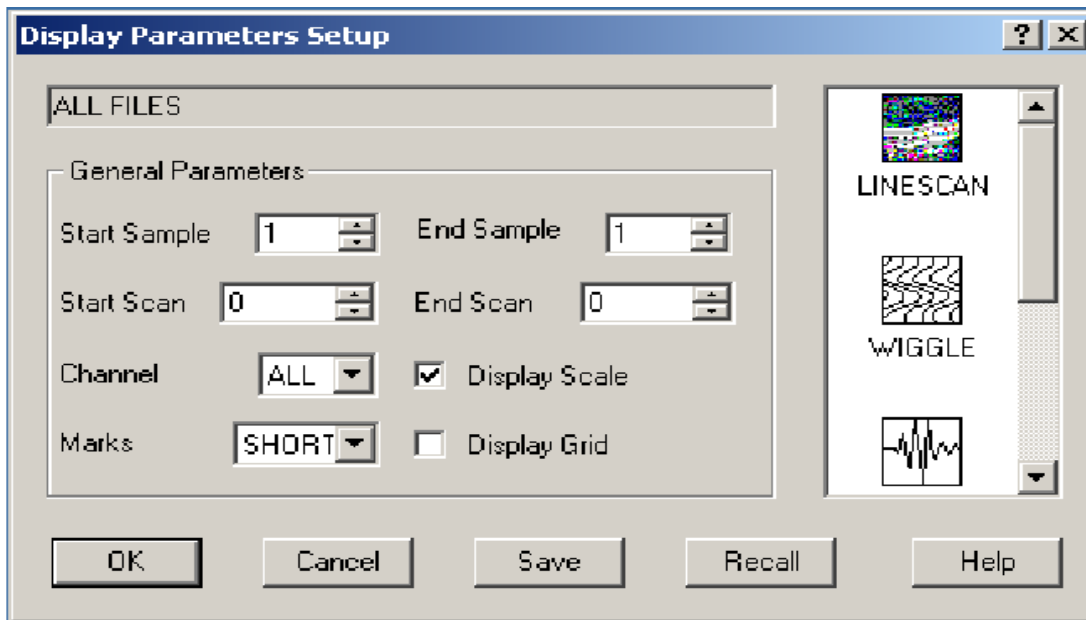
Figure 5.3. Display Parameters Setup
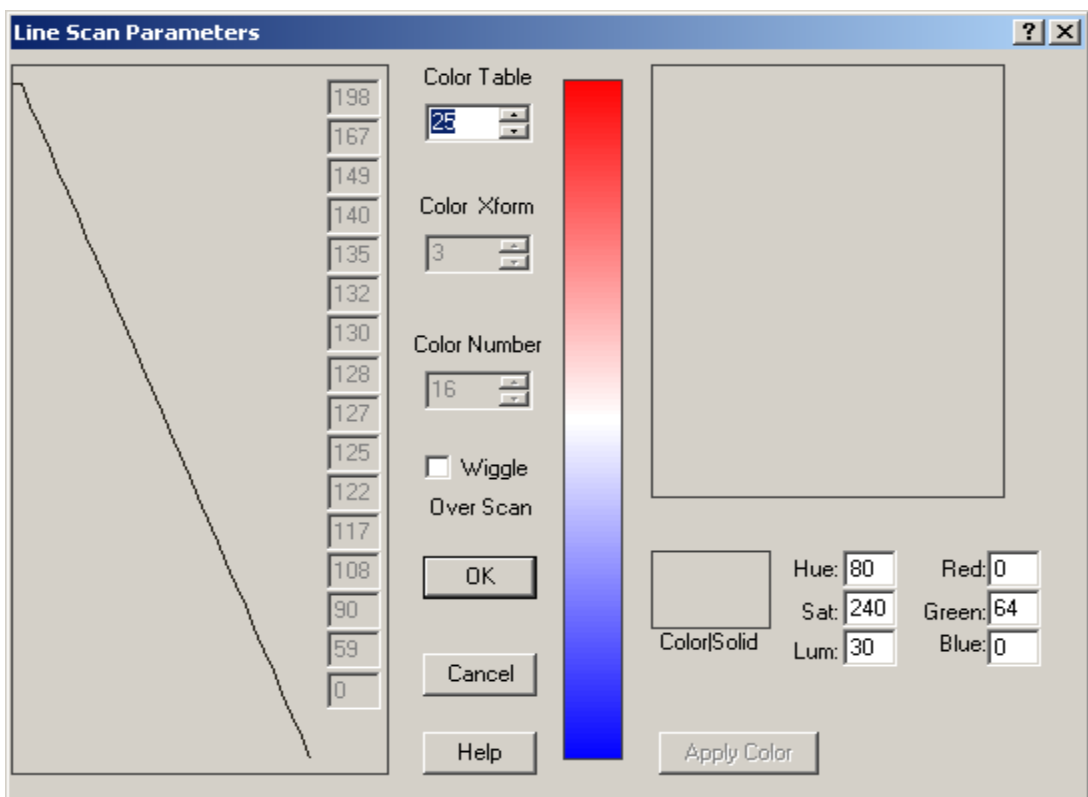
Figure 5.4. Linescan Parameters Setup Dialog Box with Color Table 25
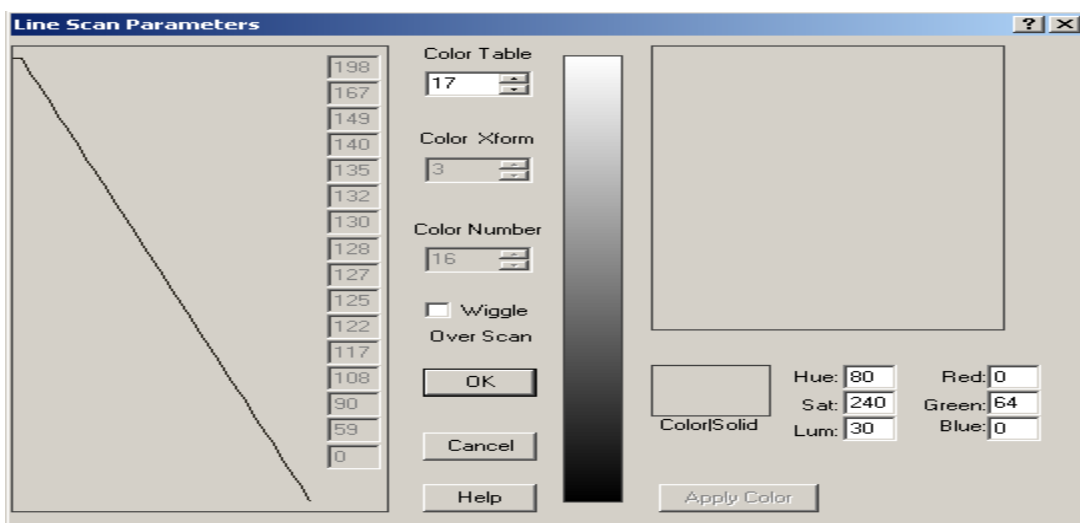
Figure 5.5. Linescan Parameters Setup Dialog Box with Color Table 17
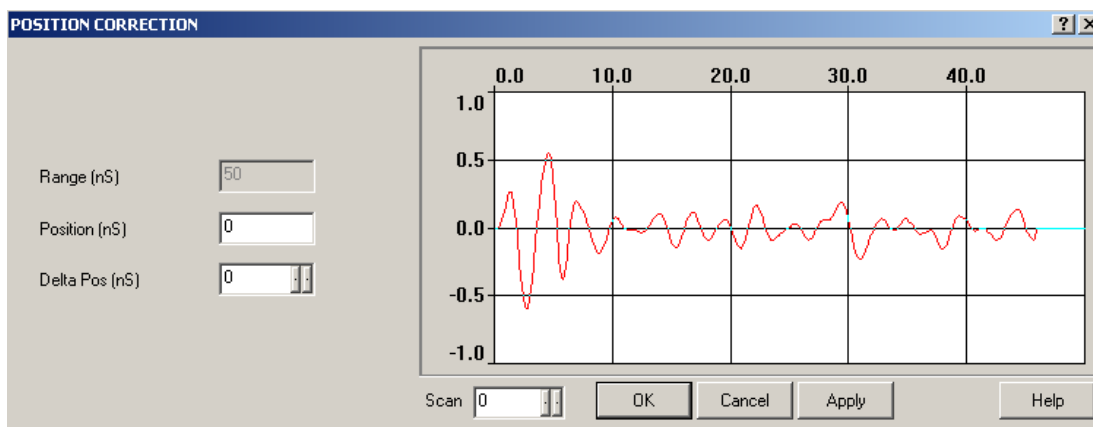
Figure 5.6. Position Setup Dialog Box (Position Correction)

In the dialog box, the position of the beginning of the trace on the time scale can be entered. The trace can also be shifted in small increments using the delta pos (nS) arrows. The scan to be displayed is selected in the scan box and can be changed by placing the mouse cursor on the display (Linescan, Wiggle, O-scope) and scrolling through the file. When you are satisfied with the correction select ok. The position correction will then be applied to the entire file. The correct 0-position is usually about 90% of the way to the first positive peak (Figure 5.7).
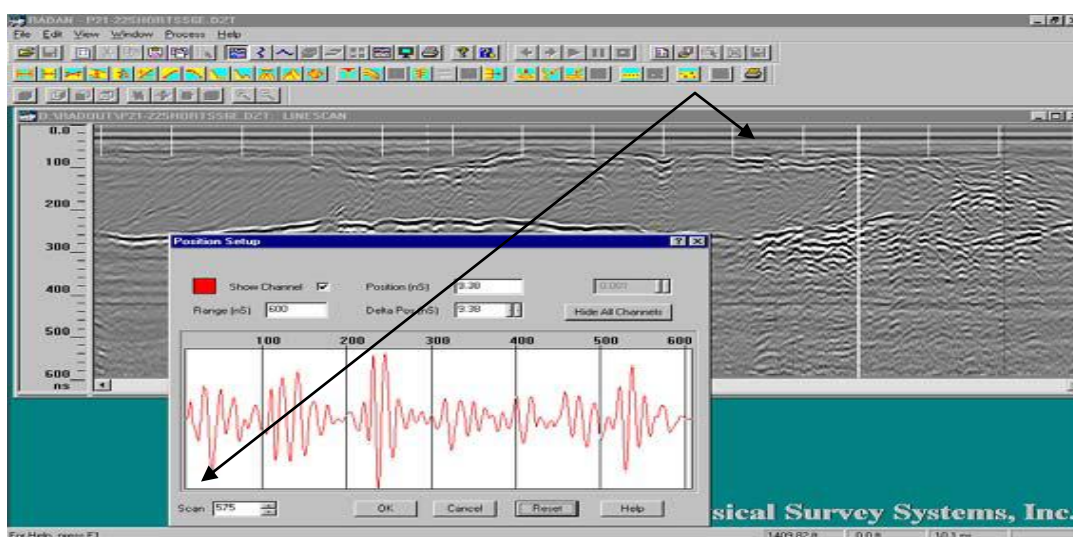
Figure 5.7. Example of the Zero Position Corrected

File header parameters include: file name, antenna frequency, range, transmitted pulse position, channel, samples/scan, bits/sample, scans/unit, units/mark, dielectric constant, and approximate depth range.

1- To open the file header choose file header under edit option "Edit > File Header" or by select the button on the toolbar.

2- Review and change as necessary the following information in the file header: Position (ns), ft/mark, scans/meter and dielectric constant.
Then used the position parameter to shift the time-zero of the vertical
scale up or down, to align it with the ground surface/top of the time window.

3- The depth parameter, if different from 0, will take priority over the dielectric-based after changes are made, choose the save button to save any changes that made to the file header.

5.6. AN EXAMPLE OF PULASKI COUNTY POOR FARM CEMETERY GPR DATA PROCESSED

In Figure 5.8 interpreted graves characterized by example weak hyperbolic shaped reflections/diffractions are shown. The GPR data of Pulaski County Poor Farm Cemetery site are poor quality (relative to what he expected and hoped for). The main reason is that; there were many obstacles (rocks, tree stumps, tree roots, irregular topography) along the traverses.

5.7. SIMILAR CASE STUDY OF A GPR IMAGE FROM VETERANS CEMETERY IN ST. JAMES

Similar case studies from one other site in Missouri were reviewed to better interpret of the acquired GPR data. Well defined hyperbolas indicative of reflections of the tops of coffins have been measured at the Veterans Cemetery in St. James Missouri.

5.7.1. Location of the Veterans Cemetery. The Veterans Cemetery is located at the Missouri Veterans Home, Saint James, Missouri, on the southeast corner of Interstate 44 and Hwy. 8. The cemetery is on the site, but it is not operated by the Federal Government. Figure 5.9 shows the photo of the Veterans Cemetery in St. James, Missouri.
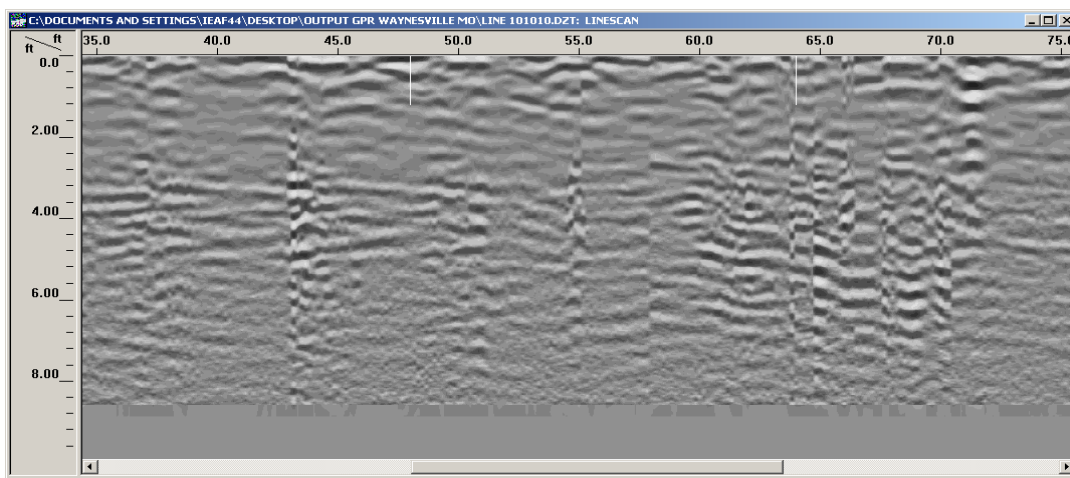
Figure 5.8. Interpreted Ground-Penetrating Radar 2D Data Processed Across Pulaski County Poor Farm Cemetery Graves (GPR Profile # 10 acquired along traverse #10)

Figure 5.9. Veterans Cemetery in St. James, Missouri

5.7.2. Interpretation of One GPR Image from Veterans Cemetery in St. James. GPR image collected at the Veterans Cemetery in St. James, Missouri is shown on Figure 5.10. This site is more nearly ideal for GPR data collection since fewer limiting factors exist at this site. The data is included here for comparison purposes and was also collected using a 400 MHz antenna. On Figure 5.10, the GPR image shows well-defined reflection/diffraction hyperbola from the top of the coffins appears to be at a depth between 1ft and 2ft.The spacing between these coffins is about 5ft, consistent with the burial practices at the Pulaski County Poor Farm Cemetery.

Figure 5.10. Ground-Penetrating Radar 2D Data Acquired Across Veterans Cemetery in St James

6. ELECTRICAL RESISTIVITY TOMOGRAPHY (ERT)

6.1. OVERVIEW OF CHAPTER SIX

This chapter is divided into five subsections. Subsection 1 is an overview of chapter six. Subsection 2 is focused on how to set up the ERT system for an automatic field survey. In subsection 3, data acquisition is covered. Subsection 4 is focused on the data processing. In subsection 5, data interpretation is discussed.
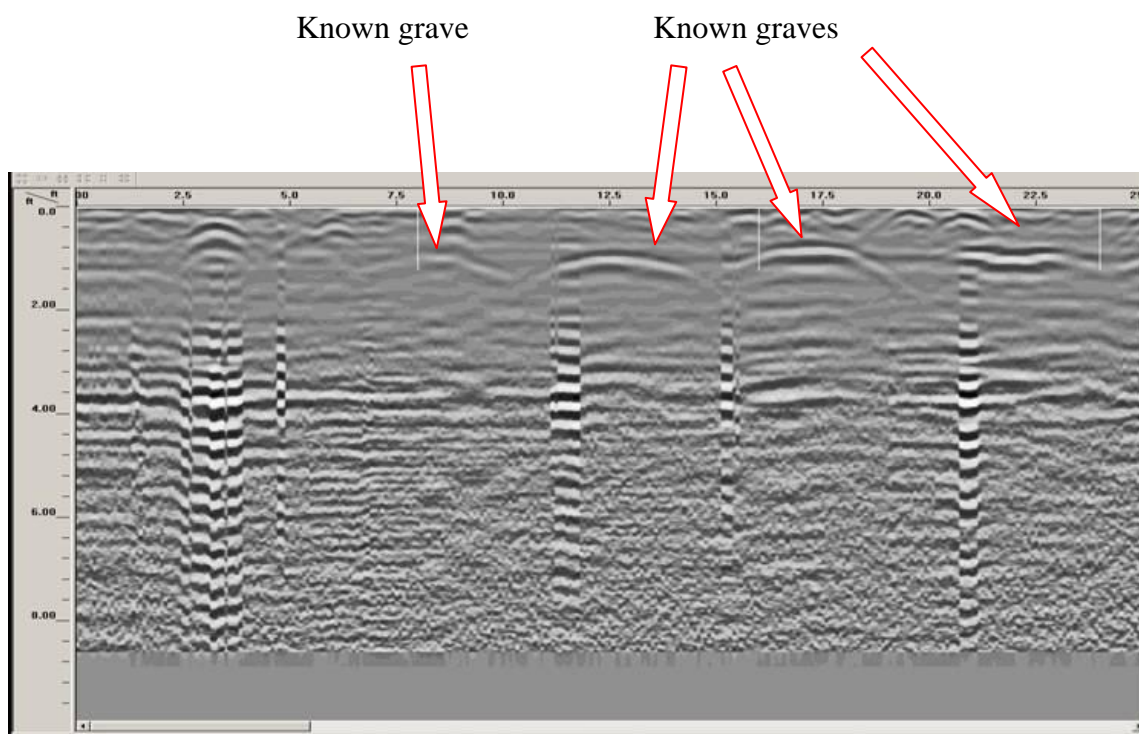
6.2. HOW TO SET UP THE SUPERSTING SYSTEM FOR AN AUTOMATIC FIELD SURVEY

The electrical resistivity system used in this survey was a Supersting R8, manufactured by Advanced Geosciences Inc. The complete field system consists of:

1. The Supersting R8 instrument console.

2. Switch boxes with passive electrode cables.

3. Stainless steel electrode stakes (68 pc).

4. 12V battery, power supply.

5. Active and passive cables.

The Supersting uses 12Volt battery. The battery is fully charged at the start of ERT survey. Figure 6.1 shows the Supersting, passive cable, active cable, the 12Volt battery. The steel stakes which conduct the current to and from the ground, number from 1 to 68.

Figure 6.2 shows how to attach the electrode switch to the stake by using the stainless steel spring. The reason why this attachment, to make sure there is metallic connection between the switch and the electrode stake. This will help to get good quality ERT data in the field survey. After the contact resistivity test was performed and no

reading on one or more electrodes, this need to double check of electrode and steel metal attachment.
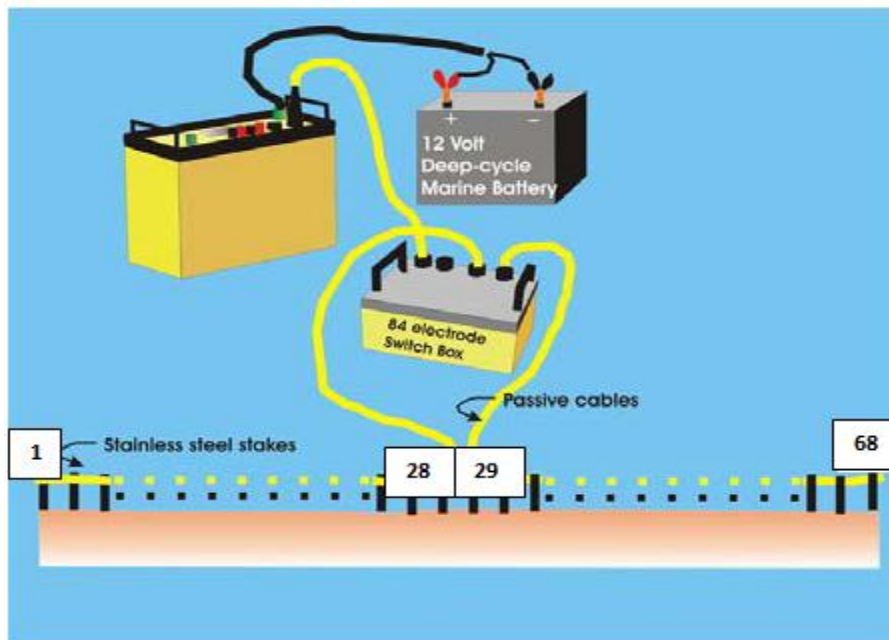

Figure 6.1. Supersting R8, Switch Box, 12V Battery, Steel Stakes

Figure 6.2. Electrode Switch Attached to the Stake

6.3. DATA ACQUISITION

• Start by stretching a tape measure along the profile line about 68ft length.

• Place the 68 stainless steel electrode stakes in the ground at 1ft spacing, on straight line.

• Lay out both the active and passive cables. Drop one switch (or take-out) at each

  stake. Note that the switches are numbered. The switch number is marked on the cable

  beside each electrode switch. The cables are laid out in the correct order so that the

  switches (take-outs in the case of passive cables) are numbered consecutively.

• Using the stainless steel springs or rubber bands, fasten each switch/take-out to its

  electrode making sure that there is metallic connection between the switch and the

  electrode stake.

• On control unit, Enter ERT file name, spacing between the electrodes (1ft), the unit

  (feet) and the last

  electrode number used in the survey (68).

• Perform contact resistivity test, and ensure that all the electrodes passed the test

  before continuing.

• Press "Measurement" bottom on control console.

6.4. DATA PROCESSING

The RES2DINV software was used to edit, correct and print the 2D model.

6.4.1. How to Run the RES2DINV Software. To run the resistivity inversion
program on the data analysis computer, click the RES2DINV icon. The program will first

check the computer system to ensure that it has the necessary resources that this program requires. It will check for the available memory and hard disc space. If the program displays a warning, quit from the program and make the necessary changes. After checking the computer configuration, the program will then display the following Main Menu bar near the top of the screen.

Select an option by clicking it with the mouse cursor. When using the program for the first time, try to read the resistivity data file xxx.dat . Then select the edit option to remove bad points and finally select the inversion option to carry out an inversion of the data set. Inversion is a process that determines the most likely physical conditions that cause the data patterns.

6.4.2. How to Read the Data File. On the RES2DINV main menu displayed on the screen as shown on Figure 6.3, click "File" option on the left top of the main menu. Submenu of "File" option will display many options. Select the first option in the submenu called "Read data file" and press enter. Now the ERT data file has been read by the RES2DINV software.
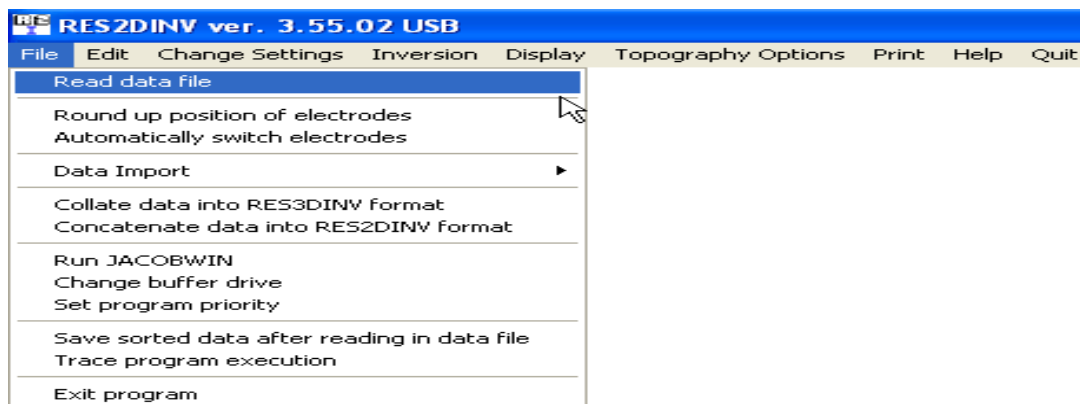
Figure 6.3. Main Menu Display of RES2DINV Software

6.4.3. Correct Bad Data Points. After ERT data has been read by RES2DINV software, check for bad data points using the "Edit" option and correct them.

Figure 6.4. Demonstration of "Edit" Option to Check and Correct for Bad Data Points

Click on "Edit" option after ERT data has been read by the RES2DINV software and then submenu will display seven options. Click the first option "Exterminate bad datum points". Figure 6.5 shows an example of a data set with a few bad data points. The data is displayed using the "Exterminate bad data points" option.
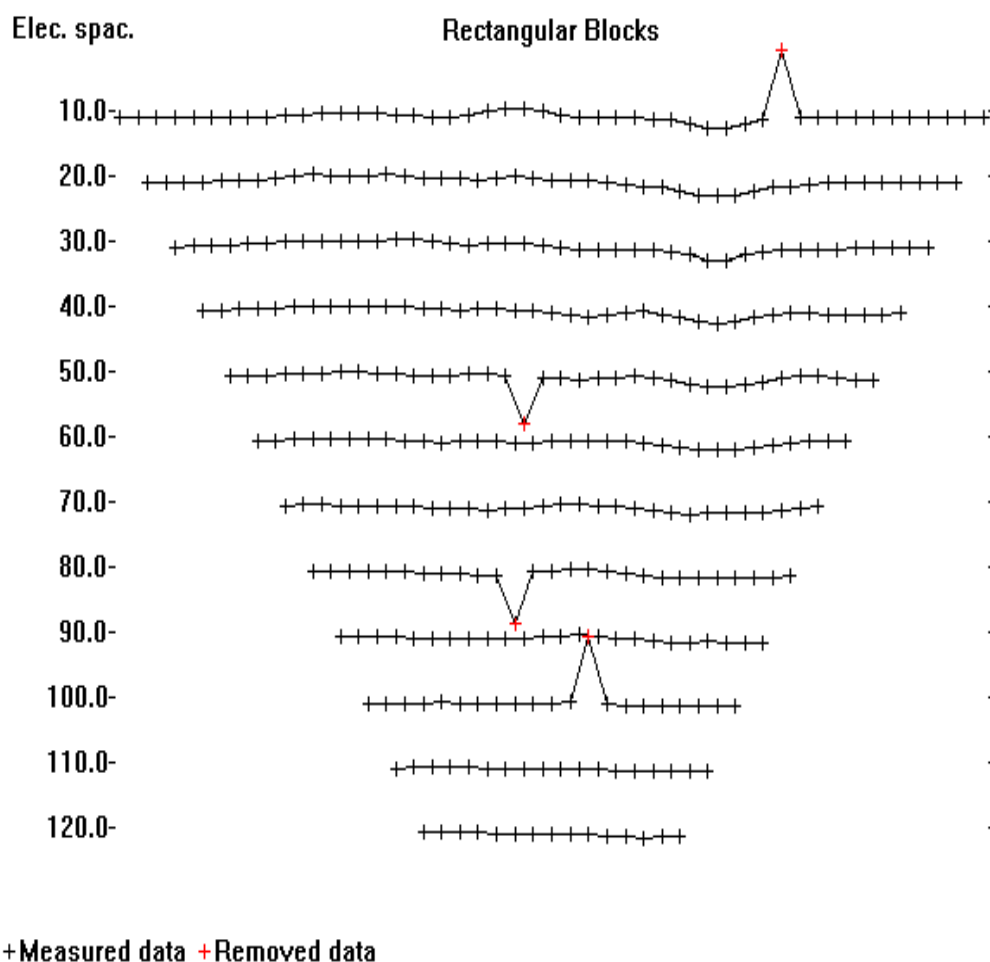
Figure 6.5. Demonstration of "Exterminate Bad Data Points" Option to Check for and Remove Bad Data Points

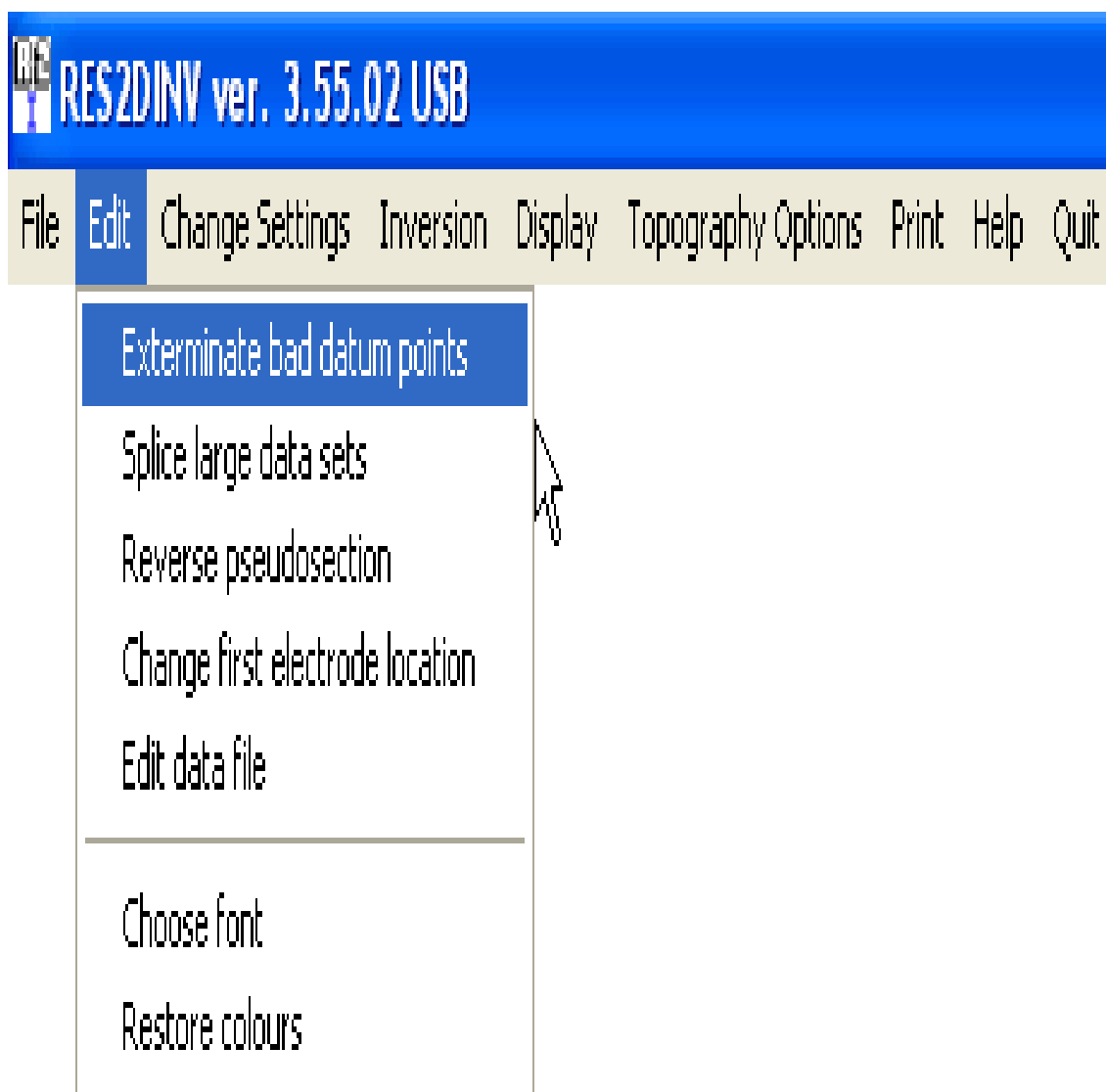**6.4.4. Inversion Options.** This is the last step of processing ERT data. Figure 6.6 shows the final step of ERT data processing. After the removal of bad data points from ERT data file, select option "Inversion" from main menu of RES2DINV software. Submenu under "Inversion" option will display; select and click the first option "Least-squares inversion" and automatically the 2D ERT model will display on the screen. The model will show the horizontal scale, vertical scale, spacing between the electrodes, and resistivity of different formations as with different colors**.**

Figure 6.6. Final Step of Processing ERT Data Using "Inversion" Option

6.4.5. 2D ERT Model. Figure 6.7 shows the final 2D ERT model along traverse 30 at Pulaski County Poor Farm Cemetery. Both horizontal and vertical scales in feet and the spacing between the electrodes was 1ft apart.
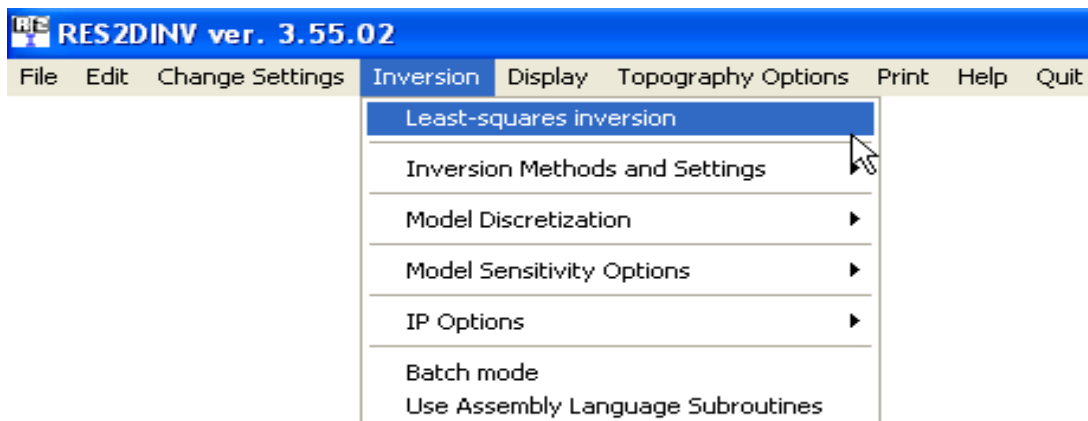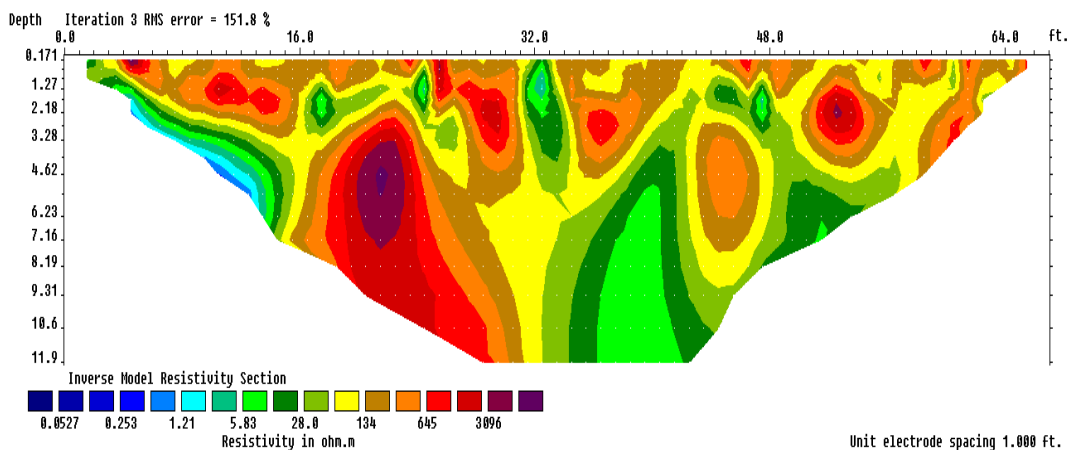

Figure 6.7. Final 2D ERT Model Along Traverse 30

7. DATA INTERPRETATION

7.1. OVERVIEW OF CHAPTER SEVEN

This chapter is divided into three subsections. Subsection 1 is overview of chapter six. Subsection 2 focused on the results and discussion, which include the maximum probable depth of penetration, a GPR data analysis of 2D GPR traverse #10 and 2D GPR traverse #41. In subsection 3, the locations of the graves are shown.

7.2. RESULTS AND DISCUSSION

7.2.1. 2D GPR Profile #10. The 2D GPR profile #10, which acquired across traverse # 10, shows five anomalies. The presence of those hyperbolic anomalies as the results of the reflected EM pulses from the top of the coffins. The five graves are located at 44ft, 49ft, 55ft and 60ft between 40ft and 75ft mark of profile #10. Hyperbolic reflections in GPR traverses are originated from localized sources and can correspond to archaeological targets (Daniels, 1996; Conyers, 2004). The shape, depth and the length of those a hyperbolic reflector are vary and this may be as the results of the collapse of the coffins or due to deterioration of the bodies. There is no direct evidence of multiple and/or overlapping graves in this GPR profile. On traverse #10, the depth to the top of the coffins is between 1.5ft and 2ft (Figure 7.1).

7.2.2 2D GPR Profile #41. This 2D GPR profile #41, which is acquired across traverse #41 shows six anomalies. The presence of those hyperbolic anomalies as the results of the reflected EM pulses from the top of the coffins. The graves are located at the 4ft, 9ft, 14ft and 19ft from the beginning of this profile. On profile #41, the depth to the top of the coffins is between 1.5ft and 2ft (Figure 7.2). The spacing between the graves about 5ft apart. This consistent with the burial practices. The shape, depth and the

length of those a hyperbolic reflector are vary and this may be as the results of the collapse of the coffins or due to deterioration of the bodies. There is no direct evidence of multiple and/or overlapping graves in this GPR profile.

Interpreted graves   **Interpreted   graves**
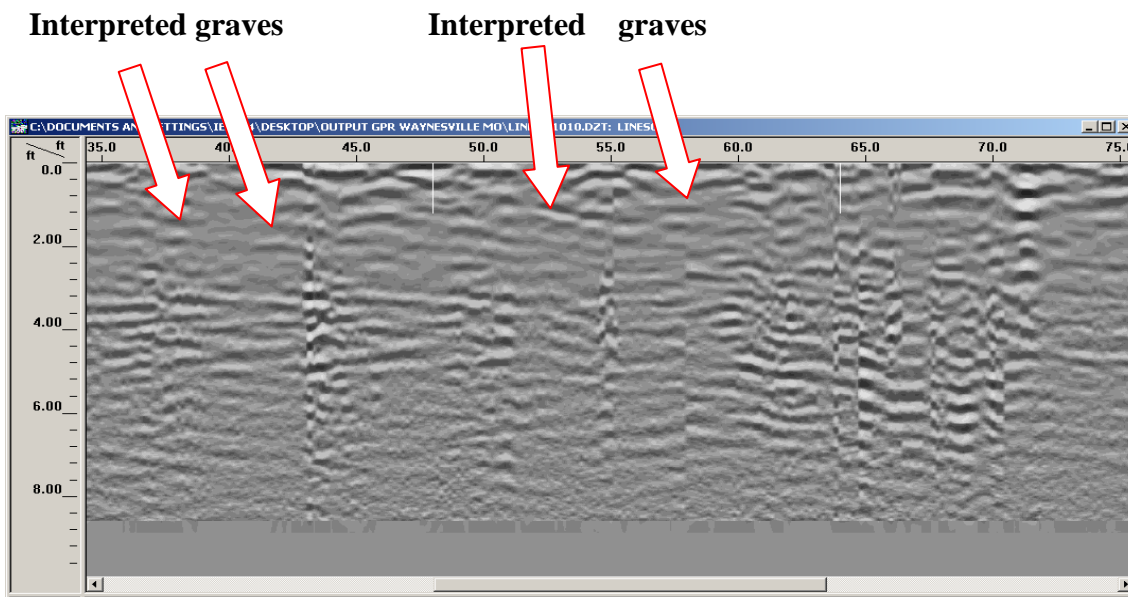

Figure 7.1. Interpreted Graves Characterized by Hyperbolic Reflectors [2D Traverse #10]

Interpreted graves   **Interpreted graves**
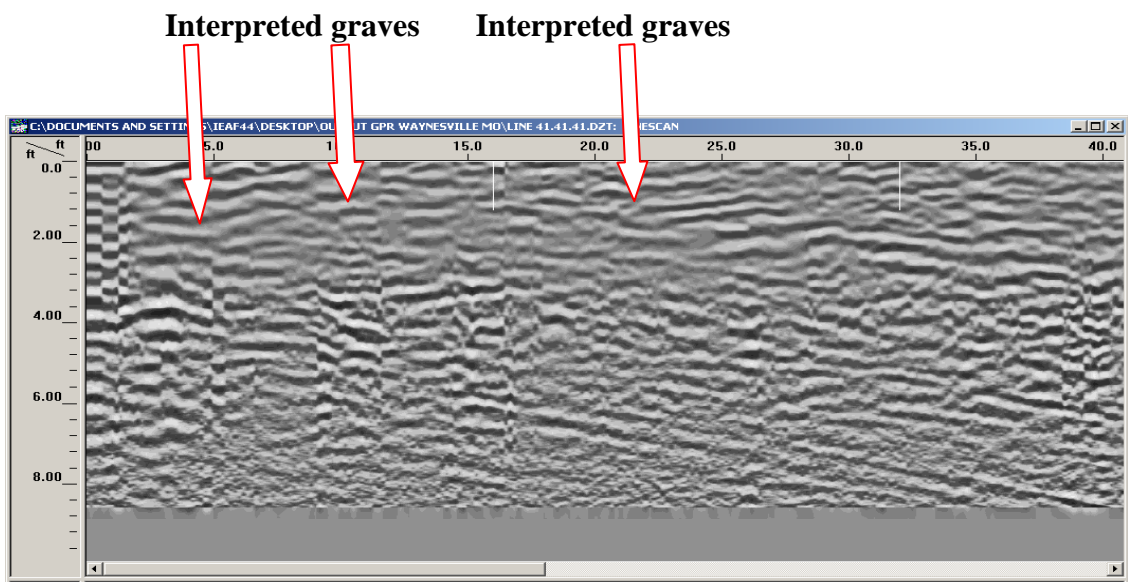
Figure 7.2. Interpreted Graves Characterized by Hyperbolic Reflectors [2D Traverse #41]

7.3. DATA INTERPRETATION

Figure 7.3 shows four high resistivity zones, A, B, C and D along traverse number 30.
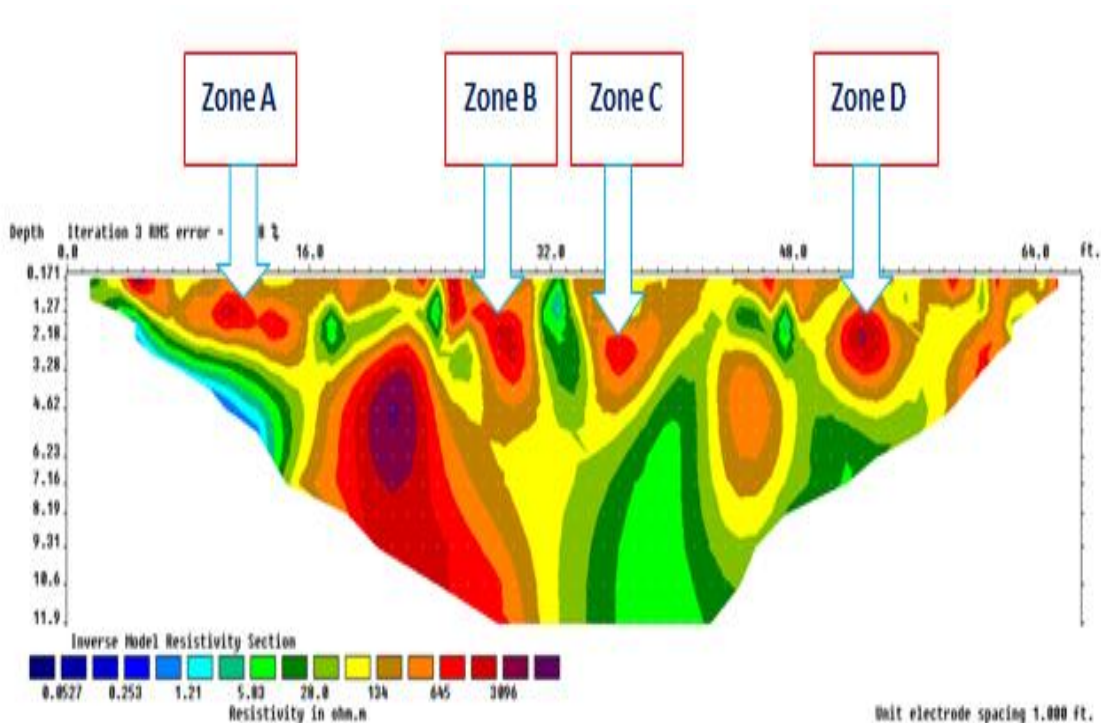
Figure 7.3. Four High-Resistivity Zones (A, B, C and D)

7.4. LOCATION OF THE GRAVE

Based on the a comprehensive visual inspection of the site, based on the interpretation of the ground penetrating radar data and based on the pattern of identifying graves on the site generated a map showing what believed the locations of all graves on the site. Understanding this interpretation it consistent with everything we could do with

the site. Accordingly there are 151 graves were found on the (Figures 7.3, 7.4, 7.5, 7.6 and 7.7).

SW ⟺ NE

Figure 7.4. Approximate Locations of Interpreted Graves (Dark Areas)

The vertical scale (Flag Numbers) corresponds to the numbers printed in black ink on the red flags that remain inserted into the ground on the site. These flags were planted

at two foot intervals. The horizontal scale is in feet. The "10 foot" mark refers to a position 10 feet from flag number 1; the "90 foot" mark refers to a position 90 feet from flag number 1. The mapped locations are based on the interpretation of variable quality GPR data. In other words this map is stretched in the NW-SE direction by a factor of about 3.6x.
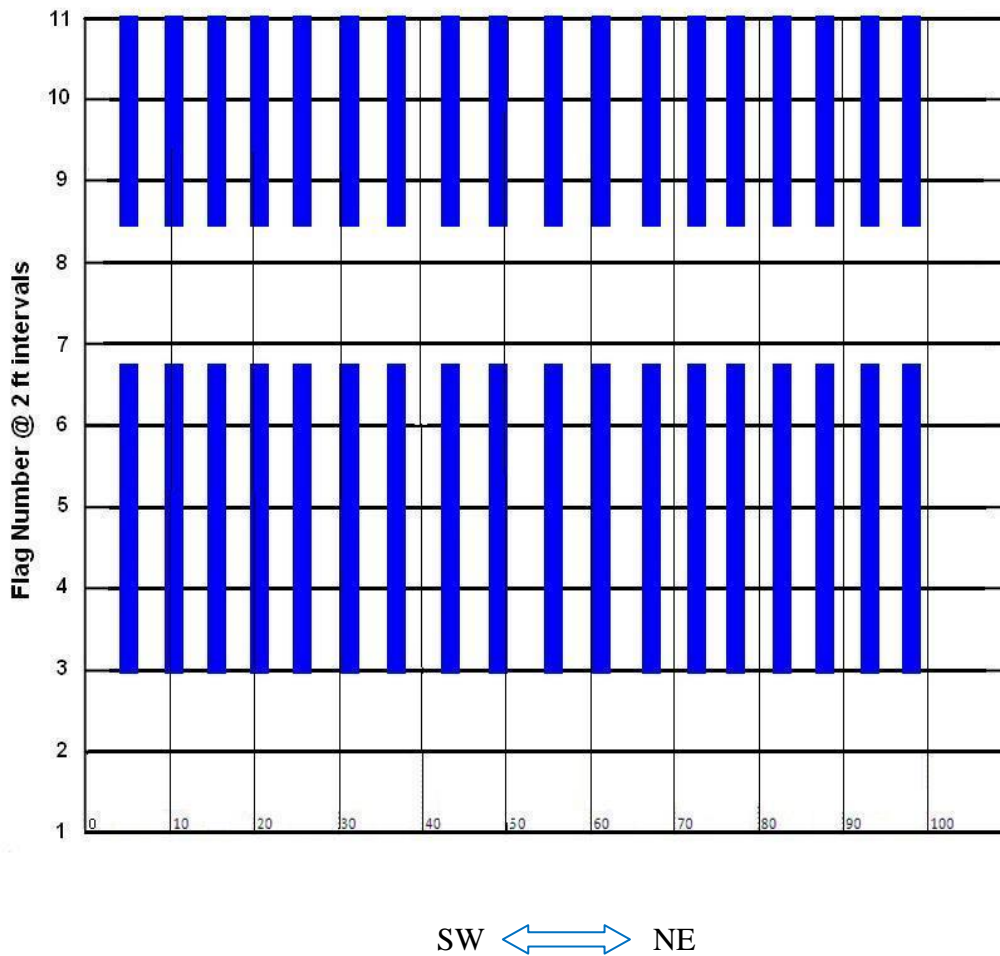

SW ⟺ NE

Figure 7.5. Approximate Locations of Interpreted Graves (Dark Areas)

The vertical scale (Flag Numbers) correspond to the numbers printed in black ink on the red flags that remain inserted into the ground on the site. These flags were planted at two foot intervals. The horizontal scale is in feet. The "10 foot" mark refers to a position 10 feet from flag number 12; the "90 foot" mark refers to a position 90 feet from flag number 12. The mapped locations are based on the interpretation of variable quality GPR data. The mapped locations are based on the interpretation of variable quality GPR data. In other words this map is stretched in the NW-SE direction by a factor of about 3.6x.
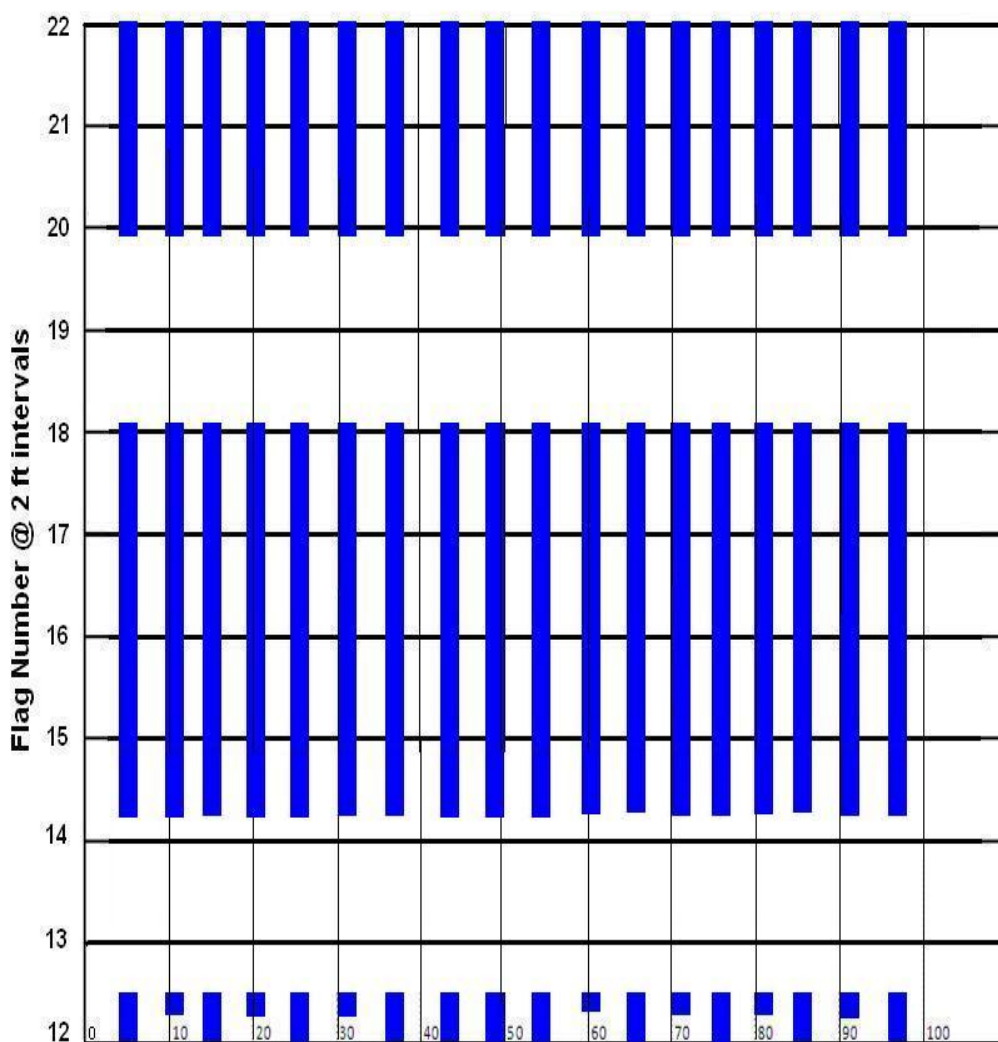

SW ⟺ NE

Figure 7.6. Approximate Locations of Interpreted Graves (Dark Areas)

The vertical scale (Flag Numbers) corresponds to the numbers printed in black ink on the red flags that remain inserted into the ground on t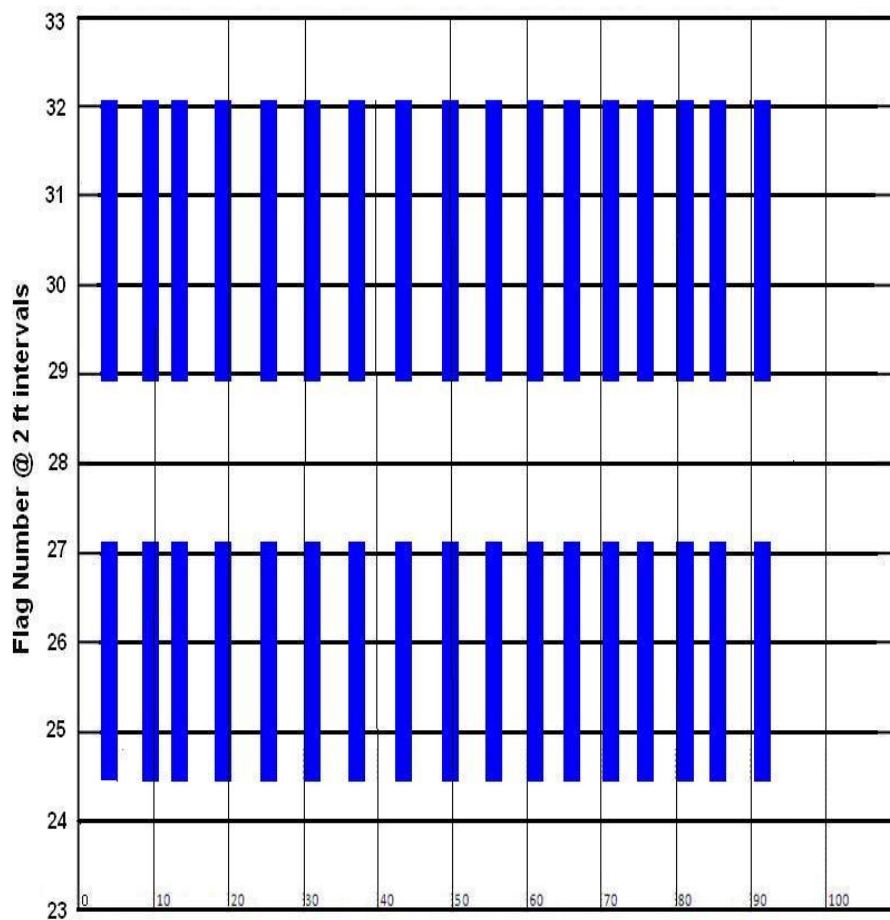he site. These flags were planted at two foot intervals. The horizontal scale is in feet. The mapped locations are based on the interpretation of variable quality GPR data. In other words this map is stretched in the NW-SE direction by a factor of about 5.4x.

SW ⟺ NE

Figure 7.7. Approximate Locations of Interpreted Graves (Dark Areas)

The vertical scale (Flag Numbers) corresponds to the numbers printed in black ink on the red flags that remain inserted into the ground on the site. These flags were planted at two foot intervals. The horizontal scale is in feet. The mapped locations are based on the interpretation of variable quality GPR data. In other words this map is stretched in the NW-SE direction by a factor of about 5.4x.
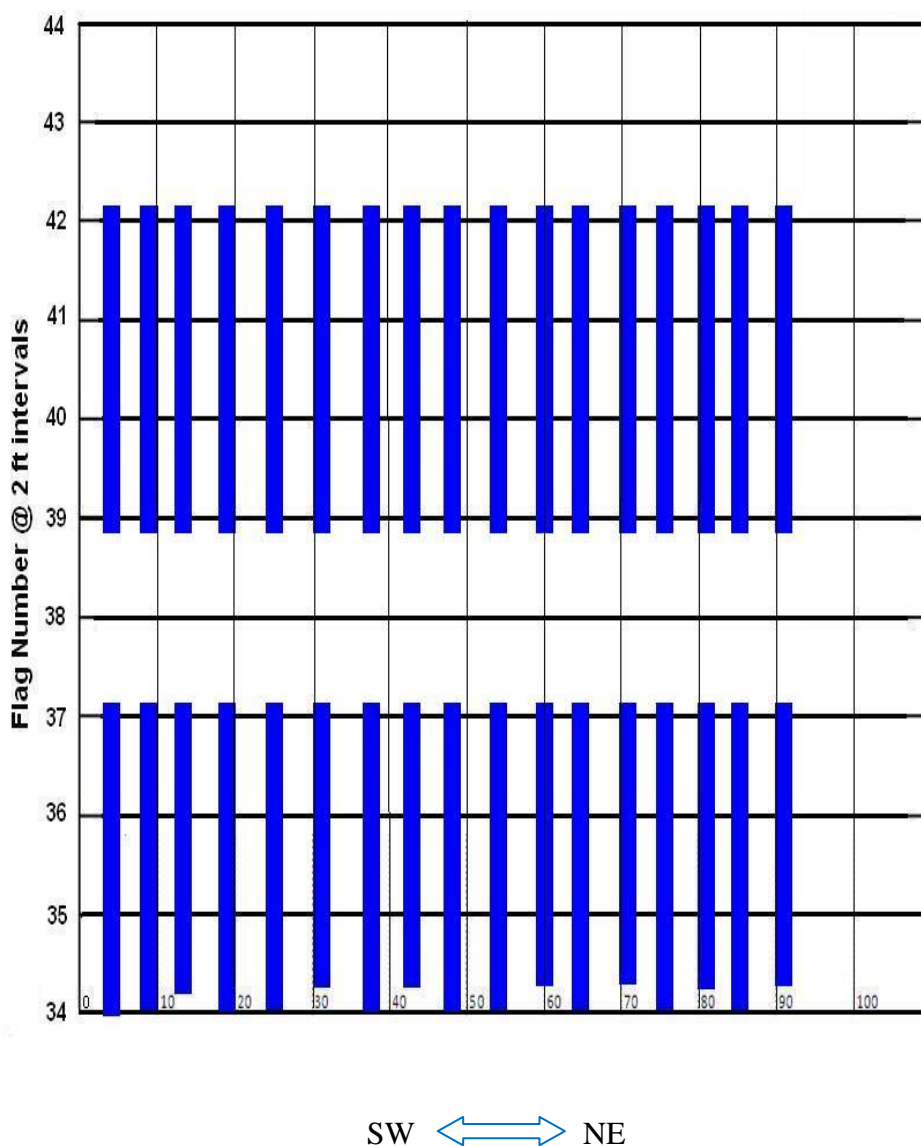

SW ⟺ NE
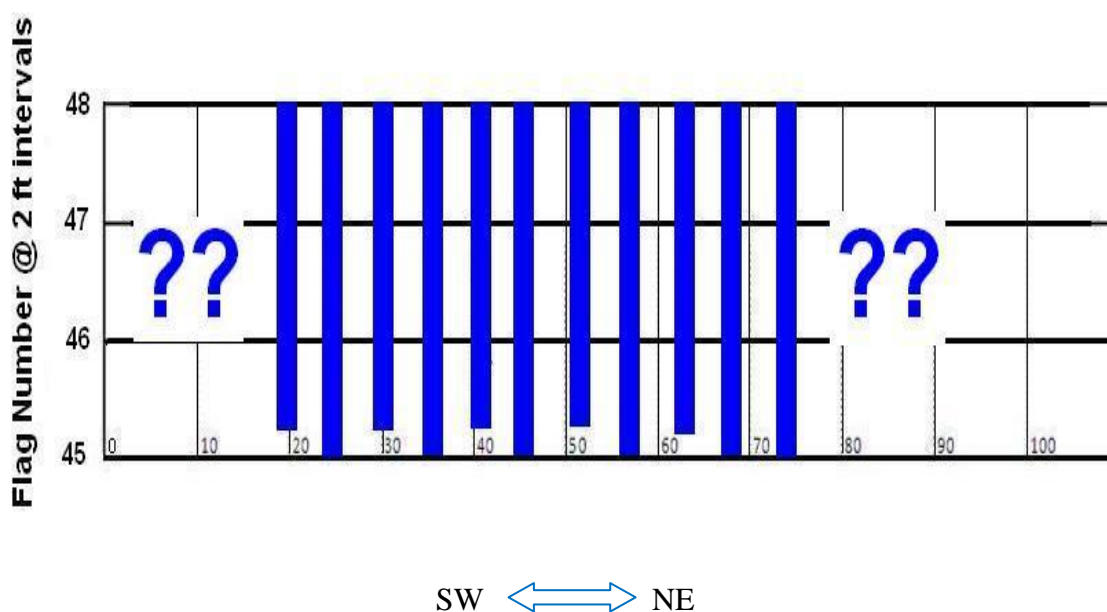
Figure 7.8. Approximate Locations of Interpreted Graves (Dark Areas)

The vertical scale (Flag Numbers) corresponds to the numbers printed in black ink on the red flags that remain inserted into the ground on the site. These flags were planted at two foot intervals. The horizontal scale is in feet. We were unable to acquire data from station "0" to station "20" on traverses 45-48, because of deadfall and standing trees.) The mapped locations are based on the interpretation of variable quality GPR data. In other words this map is stretched in the NW-SE direction by a factor of about 4.8x.

8. CONCLUSIONS AND RECOMMENDATIONS

Three techniques were used to investigate the Pulaski County Poor Farm Cemetery site: visual site inspection, ground penetrating radar (GPR) and electrical resistivity tomography (ERT). The author visited the site a total of the five times since September 12, 2010. Each time the author took additional photographs, re-mapped some of the indentations and inspected the indentations (with the expectation of each the indentation represented a grave). During the visual site inspection of the site, the land surface was examined for features indicative of burial sites. Two marked headstones were found one dated 1905, the other dated 1912. Apparently the Pulaski County Poor Farm Cemetery is at least 106 years old.

In total, eighty seven (87) surface indentations were mapped and plotted on a base map. In areas with no visible indentations, we acquired ground penetrating radar and some electrical resistivity data. Interpretation of ground penetrating radar data identified an additional sixty four (64) possible grave sites. We are very confident that each of the mapped indentations represents a grave, but are less confident of our interpretation of ground penetrating radar data, and least confident of the electrical resistivity data.

Based on visual site inspections and the interpretation of the ground penetrating radar data, the recommendation to the Pulaski County Historical Society is to place markers on each of the 151 identified potential grave sites. It is possible that a couple of these identified anomalies may be not graves. If additional data is acquired on the Pulaski County Poor Farm Cemetery site, the Society is encouraged to use a GPR with 400 MHz antenna and to remove as many obstacles like trees, tree roots and rocks as possible to improve the quality of the acquired ground penetrating radar data.

REFERENCES

Annan, A., and Cosway, S., 1994, GPR frequency selection: in, Proc. of the Fifth International Conference on Ground Penetrating Radar, June 12-12, 1994, Kitchener, Ontario, Canada, Waterloo Centre for Groundwater Research and Canadian Geotechnical Society, p. 747-760.

Basson, U., 2000. Imaging of active fault zone in the Dead Sea Rift: Evrona Fault Zone as a case study. Thesis submitted for the degree of Ph.D., Tel-Aviv University, Raymond & Beverly Sackler, Faculty of Exact Sciences, Department of Geophysics & Planetary Sciences, 196 pp.

Baker, G., Jordan, T., and Pardy, J., Introduction to Ground Penetrating Radar (GPR): Stratigraphic Analyses Using GPR, Geological Society of America, Boulder, Colorado, 2007, p. 1-18.

Daniels, D.J., 1996. Surface Penetrating Radar. Institution of Electrical Engineers, London, 300 pp.

Daniels, D.J., Ground Penetrating Radar (Lee Radar, Sonar, Navigation and Avionics Series). Stevenage, UK: Institution of Electrical Engineers, 2004 ------, Surface-Penetrating Radar, Sonar, Navigation and Avionics Series, 6) Stevenage, UK: Institution of Electrical Engineers, 1996.

Davis, J.L., and Annan, A. P., 1989. Ground penetrating radar for high resolution mapping of soil and rock stratigraphy. Geophysical prospecting, Vol. 37, p. 531-551.

Federal Highway Administration (FHWA). 2007 National Bridge Inventory (NBI). October 15, 2008.

Geophysical Survey System, Incorporated, 1995, RADAN for Windows Manual, New Hampshire.

Geophysical Survey System, Inc. GSSI Handbook for Radar Inspection of Concrete GSSI Manual # MN72-367 Rev. D. New Hampshire: Geophysical System Survey Inc, 2005.

GSSI SIR-3000 User's Manual. Salem, New Hampshire: Geophysical System Survey Inc2006. Bridge Assessment Module: RADAN 6.5 User's Manual MN 43-172 Rev C. Salem New Hampshire: Geophysical Survey Inc. 2007.

Pulaski County Historical Society. History of Pulaski County Missouri, Volume II Pulaski County Historical Society, Waynesville, 1987.

Maierhofer, C. "Nondestructive Evaluation of Concrete Infrastructure With Ground
    Penetrating Radar."Journal of Materials in Civil Engineering Volume 15, No.3
    (2003): 287-297. October 1, 2008 www.asce.org.

Reynolds, J.M. An Introduction to Applied and Environmental Geophysics. West
    Sussex, England: John Wiley & Sons Ltd, 1997.

Waynesville Daily Guide posted on August 17, 2010, Waynesville, Missouri.

VITA

Ibrahim Ahmed was born in Sagadi Garib, Almahmyia Garib Province, Sudan. He received his primary school education in Sagadi Garib's Boys Primary School and Sagadi Garib Middle School in Sagadi Garib, Sudan. He graduated from Atbara High School, in Atbara, Sudan. Mr. Ibrahim began his collegiate studies in Khartoum, Sudan and received a Bachelor of Science in Geology at Khartoum University in Khartoum, Sudan.

In January 2010 Mr. Ibrahim joined Missouri University of Science and Technology, Rolla, Missouri in Geological Engineering Program for his Master Degree and he worked about 15 subsurface applied geophysics projects, most of these projects in Missouri State, some projects in Illinois State and other in Arkansas State. The Geophysical methods we used include Ground Penetrating Radar, Electrical Resistivity Tomography, Metal Detector, Seismic Refraction and Multichannel Analysis-Surface Waves (Data Acquisition and Data Processing). He also worked as both Research and Teaching Assistant on these above mentioned geophysical methods. During fall 2011 he worked at Missouri University of Science and Technology as teaching assistant for GE 336 (Geophysics Methods-graduate level course) teaching both graduate and undergraduate students GPR labs. Finally he received his Master degree in December 2011 from Missouri University of Science and Technology in Geological Engineering at Rolla, Missouri, United States of America.